NATIONAL AERONAUTICS AND SPACE ADMINISTRATION

Technical Memorandum 33-519

Computation of Solar Wind Parameters from the OGO-5 Plasma Spectrometer Data Using Hermite Polynomials

Marcia Neugebauer

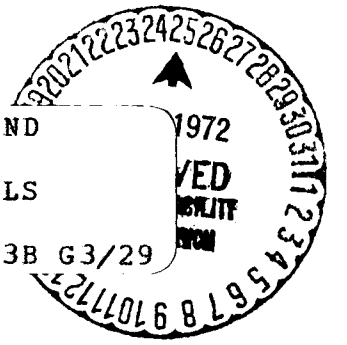

JET PROPULSION LABORATORY
CALIFORNIA INSTITUTE OF TECHNOLOGY
PASADENA, CALIFORNIA

December 15, 1971

NATIONAL AERONAUTICS AND SPACE ADMINISTRATION

Technical Memorandum 33-519

Computation of Solar Wind Parameters from the OGO-5 Plasma Spectrometer Data Using Hermite Polynomials

Marcia Neugebauer

JET PROPULSION LABORATORY
CALIFORNIA INSTITUTE OF TECHNOLOGY
PASADENA, CALIFORNIA

December 15, 1971

Prepared Under Contract No. NAS 7-100
National Aeronautics and Space Administration

PREFACE

The work described in this report was performed by the Space Sciences Division of the Jet Propulsion Laboratory.

FIGURES (contd)

CONTENTS

ABSTRACT

In this report, we present the method used to calculate the velocity, temperature, and density of the solar wind plasma from spectra obtained by attitude-stabilized plasma detectors on the earth satellite OGO 5. The method, which uses expansions in terms of Hermite polynomials, is very inexpensive to implement on an electronic computer compared to the least-squares and other iterative methods often used for similar problems in the past.

COMPUTATION OF SOLAR WIND PARAMETERS FROM THE OGO-5 PLASMA SPECTROMETER DATA USING HERMITE POLYNOMIALS

DESCRIPTION OF THE INSTRUMENTS

Ludwig (1963) has given a description of the OGO satellites. The plasma experiment reported here consists of two nearly identical packages: one looking toward the sun, and the other looking radially away from the earth. Each package contains both a curved-plate electrostatic analyzer and an ac Faraday cup.

Let us consider only the solar-oriented package. The basic concepts of its operation can be understood with the aid of the flow diagram in Fig. 1.

The Faraday cup makes high time resolution measurements of the total charge flux of those positive ions whose velocity component parallel to the satellite-sun line corresponds to an energy per unit charge (E/Q) between 100 and 11,000 volts; this range of E/Q usually includes both the protons and the α particles in the solar wind.

The average direction of positive-ion flow can be computed from the relative currents reaching each of four collectors in the Faraday cup. The details of this calculation are given in Appendix 1.

At the same time that the ions' total charge flux and direction are measured by the Faraday cup, a series of voltages is applied to the electrodes of the electrostatic analyzer to obtain the E/Q spectrum either of positive ions or of electrons. This curved plate analyzer has much in common with one flown on Mariner 2 (Neugebauer and Snyder, 1966; Graham and Vescelus, 1967). Positive ions entering the detector pass through (1) an entrance aperture at the spacecraft ground potential, (2) the cylindrical deflection electrodes, which are 120° in length and which have the ratio of the radius of curvature of the outer electrode to that of the inner electrode equal to 1.134, (3) an exit aperture at ground potential, and (4) a suppressor grid at a potential of − 12 volts with a transparency of 92%. The ions then enter a collector cup, and the current to this collector is determined by the electrometer system for each voltage setting (channel) on the deflection electrodes.

There are 128 overlapping E/Q channels equally spaced on a logarithmic scale between 2.54 volts and 16.9 kv; α particles should appear 10 channels above protons with the same velocity. A few more details about the operation of the curved plate analyzer are given in Appendix 2.

The assumption that each ion species in the plasma can be described by a Boltzmann distribution (temperature T) in a reference frame moving relative to the detector with velocity v_o in a direction given by θ_o and φ_o allows one to calculate values of T, v_o, and density n, from a spectrum. It is then possible to apply a temperature correction to the calculation of θ_o and φ_o from the Faraday cup currents and then repeat

the calculation of v_o, T, and n (see Fig. 1); however, for the ratio of thermal velocity to flow velocity usually found in the solar wind, this correction is negligible compared with other uncertainties in these angles.

Next, the apparent, or measured, total charge flux can be corrected for angle of incidence and temperature to obtain an estimate of the true total charge flux = $\Sigma q_i n_i v_i$, where the sum is taken over all species of positive ions.

It is known that all species of ions in the solar wind have approximately the same velocity (Bame et al., 1968; Ogilvie et al., 1968) and that the solar wind is electrically neutral (Montgomery et al., 1968). Thus, $(\Sigma q_i n_i v_i)/v = n_e$, the electron number density.

The electron number density can also be calculated by summing the positive-ion $q_i n_i$ as determined from the curved-plate analyzer spectra. However, a large thermal anisotropy, which has often been observed in the solar wind (Scarf et al., 1967; Hundhausen et al., 1967) will introduce a greater error into this method than into the method using the total charge-flux measurements.

METHOD OF COMPUTING PLASMA PARAMETERS FROM CURVED PLATE ANALYZER SPECTRA

The current $\mathcal{J}$ measured by the electrometer of the curved plate analyzer when the voltage across the plates is set for channel I is given by

$$\mathcal{J}(I) = qA \iiint g_1(\theta)\; g_2\left(\frac{v}{v_I}, \varphi\right) v \cos\theta \cos\varphi \; f(v,\theta,\varphi)\; d^3v \qquad (1)$$

where:

q = charge of the incoming ion

A = effective detector aperture area = 2.26 cm^2

v = velocity of the ion

v_I = velocity at center of channel I

The angles θ and φ are defined as shown in Fig. 2. In this coordinate system

$$d^3v = v^2 \cos\theta \, d\theta \, d\varphi \, dv \quad . \tag{2}$$

The product $g_1(\theta)\, g_2(v/v_I,\varphi)$ is the response function of the analyzer.

$$\begin{aligned} g_1(\theta) &= 1 + \theta/10.1^\circ \quad \text{for } \theta \le 0^\circ \\ &= 1 - \theta/10.1^\circ \quad \text{for } \theta \ge 0^\circ \\ &= 0 \qquad\qquad\quad \text{for } |\theta| > 10.1^\circ \end{aligned} \tag{3}$$

The function $g_2(v/v_I,\varphi)\cos\varphi$ was determined experimentally by calibration with a cold argon ion beam of large cross-section. This function is plotted in Fig. 3.

$f(v,\theta,\varphi)$ is the distribution function of the ions. If we assume the particles have an isotropic Boltzmann distribution superimposed on a convection velocity of magnitude v_o and direction given by θ_o and φ_o,

$$f(v,\theta,\varphi) = n\left(\frac{m}{2\pi kT}\right)^{\frac{3}{2}} e^{-m|\vec{v}-\vec{v}_o|^2/2kT} \tag{4}$$

$$\begin{aligned} |\vec{v}-\vec{v}_o|^2 = v^2 + v_o^2 - 2v\, v_o[&\cos\theta\cos\varphi\cos\theta_o\cos\varphi_o \\ &+ \cos\theta\sin\varphi\cos\theta_o\sin\varphi_o + \sin\theta\sin\theta_o] \end{aligned} \tag{5}$$

When Eqs. (2) through (5) are substituted into Eq. (1), the θ integral can be done either analytically (if it is assumed that θ is a small angle) or numerically (for any θ). The φ and v integrals have been done numerically. The result is

$$\mathcal{J}(I) = qA\ n\ v_o\ G[\nu(I),\theta_o,\varphi_o,\xi]$$

where

$$\nu(I) = \log\ (v_I/v_o)$$

$$\begin{cases} v_I = \text{velocity at center of channel I} \\ v_o = \text{convection velocity} \end{cases}$$

$$\xi = \log\left(\frac{mv_o^2}{2kT}\right)$$

Examination of many computed values of G suggested it could be rewritten as

$$G[\nu(I),\theta_o,\varphi_o,\xi] = \left\{T[\nu(I),\varphi_o,\xi] \equiv G[\nu(I),0,\varphi_o,\xi]\right\} \times 10^{-\theta_o^2 G_1(\xi)}$$

A least-squares fit of the function

$$\frac{1}{\theta_o^2}\log\frac{G[\nu(I),\theta_o,\varphi_o,\xi]}{G[\nu(I),0,\varphi_o,\xi]}$$

to a power series in ξ gives

$$G_1(\xi) = (5.05006 - 10.6985\ \xi + 8.62214\ \xi^2 - 1.506114\ \xi^3) \times 10^{-3}$$

for θ_o in degrees.

$T[\nu(I),\varphi_o,\xi]$ has been computed and tabulated as TAB(I,J,L):

I = 1 to 16 for $\nu(I) = [-\ 8\ \log\ 2^{.05} = -\ .12041]$ to $[+\ 7\ \log\ 2^{.05} = .10536]$ in steps of $\Delta\nu(I) = \log\ 2^{.05} = .015052 = 1$ channel.

J = 1 to 11 for φ_o = - 10° to + 10° in steps of $\Delta\varphi_o$ = 2°

L = 1 to 10 for ξ = 1.2 to 3.0 in steps of $\Delta\xi$ = 0.2

Appendix 3 is a listing of TAB(I,J,L). [Note: A minor goof resulted in each value of the array TAB(I,J,L) being too big by a factor of 2. This was taken into account when calculating density.]

In computing the plasma parameters corresponding to a measured series of $\mathcal{J}(I)$ (i.e., a spectrum), it is assumed that the angles θ_o and φ_o are known from the Faraday cup measurements. A computer program was written to find the values of n, v_o, and $\xi = \log(\ mv_o^2/2kT)$ which minimized the function

$$\sum_I \left[\mathcal{J}(I) - qA\ n\ v_o\ 10^{-\theta_o^2 G_1(\xi)}\ T\left(\frac{v_I}{v_o}\ ,\varphi_o,\xi\right)\right]^2$$

The computations were iterative and time consuming. Thus we wrote a second computer program which computes n, v_o, and ξ by comparing the coefficients of the Hermite polynomials of the measured and the theoretical spectra; it is a relatively quick, non-iterative calculation.

HERMITE POLYNOMIALS

A function w(x) which is shaped sort of like a Gaussian, can be expanded in a series of Hermite polynomials as:

$$w(x) = \frac{C_o}{\sigma\sqrt{2\pi}}\, e^{-(x-\bar{x})^2/2\sigma^2}\left[1 + \sum_{i=3}^{n} \frac{C_i}{i!}\, H_i\left(\frac{x-\bar{x}}{\sigma}\right)\right]$$

where the Hermite polynomials of order 3 and 4 are

$$H_3(x) = x^3 - 3x$$

$$H_4(x) = x^4 - 6x^2 + 3$$

and in general $H_{n+1}(x) = x\,H_n(x) - H_n'(x)$

$$= x\,H_n(x) - n\,H_{n-1}(x)$$

The low order coefficients can be expressed in the following form:

$$C_o = \int_{-\infty}^{\infty} w(x)\,dx$$

$$C_1 \equiv \bar{x} = \frac{1}{C_o}\int_{-\infty}^{\infty} x\,w(x)\,dx$$

$$C_2 \equiv \sigma^2 = \frac{\int_{-\infty}^{\infty} x^2\,w(x)\,dx}{C_o} - C_1^2$$

$$C_3 = \frac{1}{C_2^{3/2}}\left[\frac{1}{C_o}\int_{-\infty}^{\infty} x^3\,w(x)\,dx - 3C_1C_2 - C_1^3\right]$$

$$C_4 = \frac{1}{C_2^2}\left[\frac{1}{C_o}\int_{-\infty}^{\infty} x^4\,w(x)\,dx - 4C_1C_2^{3/2}C_3 - 6C_1^2C_2 - C_1^4\right] - 3$$

DISCUSSION OF THE METHOD

The method used to compute the plasma parameters via Hermite polynomials consists of:

1. Using the measured spectrum to compute the Hermite coefficients C_o^m through C_4^m, where the superscript m refers to measured values.

2. For the angle of incidence determined by the Faraday cup, computing a set of coefficients C_o^t through C_4^t for each of the 10 values of the parameter ξ in the comparison table, where the superscript t refers to theoretical values.

3. Finding the value of ξ for which $C_2^m = C_2^t$.

4. Using ξ from step 3, C_o^m, C_1^m, $C_o^t(\xi)$, and $C_1^t(\xi)$ to directly compute v_o, T, and n.

5. Using C_o^m through C_4^m to fit a curve through the measured spectrum and then compute the relative variance of the measurements from the curve.

6. Computing the differences $C_3^m - C_3^t(\xi)$ and $C_4^m - C_4^t(\xi)$ as measures of the excess skew and excess kurtosis, respectively, to tell in what directions the measured spectra differ from spectra corresponding to convected Boltzmann distributions.

The principal complication, which is glossed over in the above outline, arises because the Hermite polynomials are orthogonal over the interval $-\infty$ to $+\infty$, whereas the measured data cover a limited range of energy which often does not even include all important contributions to the peak. On OGO 5, the number of points/spectrum were limited by (1) only allowing 4 channels above the peak channel, to avoid contamination by heavier ions, (2) the finite noise level of the electrometer, and (3) at high bit rates, the first current measurements following a switch from the low to high sensitivity scales of the electrometer could not be used. We get the best results when the energy range used to compute the C_o^t through C_4^t in step 2 is truncated to match the energy range of the

measured spectrum as closely as possible, rather than using the entire energy range over which TAB(I,J,L) > 0.0000.

COMPUTATION OF COEFFICIENTS OF MEASURED SPECTRUM

A spectrum consists of current measurements in 1 to 8 channels below the channel with the largest current (the "peak channel") plus 1 to 4 channels above the peak channel; no more channels are taken above the peak channel to avoid contamination by heavier ions (for OGO-5, the alpha peak is expected to be 10 channels above the proton peak). To compute the Hermite coefficients for a measured spectrum, the independent parameter x is chosen to be the difference in channel number: x(I) = (channel number of measurement I) - (peak channel number), and the function w is the measured current $\mathcal{J}(I)$. Then the first five Hermite coefficients are calculated as follows:

$$C_o^m = \int_{-\infty}^{\infty} w(x)\, dx \approx \sum_I \mathcal{J}(I) * A(I)$$

where the A(I) = 1, 2, or 4, according to Simpson's rule of numerical integration.

$$C_1^m = \frac{1}{C_o^m} \sum_I [\mathcal{J}(I) * X(I) * A(I)] = \bar{x}$$

$$C_2^m = \frac{1}{C_o^m} \sum_I [\mathcal{J}(I) * X(I)^2 * A(I)] - (C_1^m)^2 = \sigma^2$$

$$C_3^m = \frac{1}{(C_2^m)^{3/2}} \left[\frac{1}{C_o^m} \sum [\mathcal{J}(I) * X(I)^3 * A(I)] - 3C_1^m C_2^m - (C_1^m)^3 \right]$$

$$C_4^m = \frac{1}{(C_2^m)^2}\left[\frac{1}{C_o^m}\sum_I [\mathcal{J}(I) * X(I)^4 * A(I)] - 4C_1^m * (C_2^m)^{\frac{3}{2}} * C_3^m - 6(C_1^m)^2 * C_2^m - (C_1^m)^4\right] - 3$$

COMPUTATION OF COEFFICIENTS FOR COMPARISON WITH MEASURED VALUES

First, note that the position and shape of the spectra depend only on the function $T(v_I/v_o,\varphi_o,\xi)$, represented in the computer by TAB(I,J,L). The factor $qAnv_o\ 10^{-\theta_o^2 G_1(\xi)}$, on which the amplitude of the spectra depend, will be worried about later. Thus, the first step in finding the theoretical coefficients to compare with the C^m is to interpolate TAB(I,J,L) to find a two-dimensional table TA(I,L) for the value of φ_o determined by the Faraday cup. Then, for each value of the unknown parameter ξ (index L in the table), we compute the $C_o^t(L)$ as follows:

1. Using the measured currents in the peak channel and the channels on either side of the peak, interpolate to find the channel number of the "peak" of the measured spectrum. If $\mathcal{J}(max)$ is the largest current measurement

$$x(peak)^m = \frac{\mathcal{J}(max+1) - \mathcal{J}(max-1)}{2[2\mathcal{J}(max) - \mathcal{J}(max+1) - \mathcal{J}(max-1)]}$$

2. Similarly, find the peaks of the theoretical spectra in the comparison table:

$$x(peak,L)^t = \frac{TA(LP+1,L) - TA(LP-1,L)}{2[2TA(LP,L) - TA(LP+1,L) - TA(LP-1,L)]}$$

where LP is the value of I for which TA(I,L) is greatest.

3. Then, the values of x_i which we wish to use in computing the Hermite coefficients are given by

$$x_i = LP + x(peak,L)^t - max - x(peak)^m + i$$

4. Interpolate the TA(I,L) to find its values at each x_i; call these values TH(IX,L).

5. $C_o^t(L) = \sum_{IX} TH(IX,L) * A(IX)$ where the A(IX) are again the Simpson's rule coefficients.

The equations for the higher order theoretical coefficients $C_1^t(L)$ through $C_4^t(L)$ are exactly like those for the measured coefficients C^m, except that TH(IX,L) is used in place of $\mathcal{S}(I)$, with the summation being over the IX.

CALCULATION OF VELOCITY AND TEMPERATURE

Next, we perform an inverse interpolation to find the value of ξ at which $C_2^t(L)$ equals C_2^m. Then, interpolate the $C_1^t(L)$ to find the value of C_1^t corresponding to this ξ. The relation between C_1^m, $C_1^t(\xi)$, and the channel number corresponding to the flow velocity v_o is perhaps made clearer by the diagram in Fig. 4, together with reminders that the TA(I,L) were defined such that $v_I/v_o = 1$ when I = 9, that the maximum values of TA(I,L) are at I = LP (LP usually = 8, 9, or 10, except when the angle is very large), and that C_1^m is the $\bar{x}$ or center of the measured spectrum relative to the observed peak channel. From Fig. 4 we see that x^* = (channel number corresponding to v_o) = {peak channel number + $C_1^m - C_1^t(\xi)$ - [LP + $x(peak,L)^t$]$_\xi$ + $x(peak)^m$ - 9} where the subscript ξ implies interpolation of the function within [ ] to the value ξ.

For OGO 5, the conversion of x^* to velocity in km/sec is given by:

$$v_o = 10^{1.32804 + 0.015052(x^* - \Delta)}$$

where $\Delta = 0$ for protons and 10 for alpha particles. Temperature in $^\circ K$ is given by

$$T = 60.5\ v_o^2\ M/10^{\xi}$$

where M = 1 for protons and 4 for alphas.

CALCULATION OF DENSITY

To find density, interpolate the $C_o^t(L)$ to find the value corresponding to ξ. Then,

$$n = \frac{1.08 * C_o^m * 10^{-\theta_o^2}\ G_1(\xi)}{Q * C_o^t(\xi) * v_o}$$

where Q = 1 for protons and 2 for alphas. The constant $1.08 = \frac{2K}{eA} \times 10^{-5}$ where the factor $K = 10^{-14}/.512$ converts the measured currents from telemetry digits into amperes (all C^m were computed from the digital output of the telemetry system, which is directly proportional to the collected currents); $e = 1.6 \times 10^{-19}$ amp; A is the effective detector area = 2.26 cm^2; the factor 10^5 converts v_o in km/sec to cm/sec; and the factor 2 corrects for the error in TAB(I,J,L) mentioned earlier.

GOODNESS OF FIT PARAMETERS

The following three parameters are computed to measure the goodness of fit of the convected Boltzmann model to the measured data:

1. The relative variance of the data from the polynomial fit

$$= \sum_I \left\{ \vartheta(I) - \frac{C_o^m}{\sqrt{2\pi C_2^m}} \, e^{-(I-I_p-C_1^m)^2/2C_2^m} \left[1 + \frac{C_3^m}{6} H_3\left(\frac{I-I_p-C_1^m}{\sqrt{C_2^m}} \right) \right.\right.$$

$$\left.\left. + \frac{C_4^m}{24} H_4\left(\frac{I-I_p-C_1^m}{\sqrt{C_2^m}} \right) \right] \right\}^2 \Bigg/ \sum_I \vartheta(I)^2$$

where I = channel number and I_p = peak channel number.

2. The excess skew = $C_3^m - C_3^t(\xi)$.

3. The excess kurtosis = $C_4^m - C_4^t(\xi)$.

Excess skew can arise when the actual distribution function rises more rapidly and decays more slowly with increasing energy than a convected Boltzmann distribution; i.e., a high energy tail would give a positive value of excess skew. Figure 5 shows the effect of a large amount of excess skew (ESKEW) for a typical (but hypothetical) spectrum with φ_o = 4°, ξ = 2.0, and with three points each above and below the peak channel.

The spectral distortions due to excess kurtosis (EKURT), or curvature, are shown in Fig. 6.

ACCURACY OF THE METHOD

As a check on the accuracy of the method, we have fit a selection of 28 spectra by both methods — least squares (LS) and Hermite polynomials (HP). The results of these computations are given in Table 1. The values of v, T, and n given are those determined by the least-squares fit. The Δv, ΔT, and Δn are the Hermite polynomial values minus the least square values. The LS error is defined somewhat differently than is the HP error, but to a first approximation they both represent the variance of the data

from the curves. The HP error is always exaggerated because the truncated energy range used in computing the Hermite coefficients leads to a poor fit (underestimation) at the fringes of the spectrum: this effect does not necessarily lead to poor estimates of the plasma parameters because of the pains taken to truncate the theoretical spectra to match the measured spectra. This effect is illustrated by the fit of spectrum #1, shown in Fig. 7. For this spectrum, $\Delta v/v = 0$, $\Delta T/T = 0.007$, and $\Delta n/n = 0.024$; i.e., there was very close agreement between the LS and the HP determined parameters despite the apparently poor fit of the HP curve.

In comparing the fits of the other spectra, we note that $|\Delta v/v|$ was less than 0.02 for all cases and was less than 0.01 for all but one spectrum. The agreement of the temperatures computed by the two methods is poorer than for the velocity. Of the 28 spectra, five had $|\Delta T/T| > 0.20$. One of these, spectrum #22, for which $\Delta T/T = 0.230$, was only 3 channels wide and had a huge HP error. The HP method is not well suited to 3-point spectra. The other four spectra are plotted in Figs. 8a through 8d; they were all weird shaped spectra. In the case of spectrum #18, the HP values of velocity and temperature are probably more realistic than the LS values.

A large value of $|\Delta T/T|$ can arise from a poor fit with either the LS method, the HP method, or both. In Figs. 9 and 10, $|\Delta T/T|$ is plotted vs. the LS error and the HP error, respectively. Both plots show some correlation between $|\Delta T/T|$ and error, which confirms again that for smooth, well shaped spectra, the HP method gives satisfactory results.

The average values of $|\Delta v/v|$, $|\Delta T/T|$, and $|\Delta n/n|$ for the 28 spectra are 0.003, 0.109, and 0.062, respectively. However, the 28 spectra were

selected so as to get a wide variety of different spectra; a random sampling would probably give appreciably smaller average differences.

COMPUTER PROGRAM

The Fortran subroutines used to perform the HP fit are given in Appendix 4, together with commentary translating the program to the notation of the text.

REFERENCES

Bame, S. J., A. J. Hundhausen, J. R. Asbridge, and I. B. Strong, Solar wind ion composition, Phys. Rev. Lett., 20, 393-395, 1968.

Graham, R. A., and F. E. Vescelus, OGO-E plasma spectrometer, Proc. Thirteenth Nat. Instrum. Soc. Amer. Aerosp. Instrum. Symp., 111-153, 1967.

Hundhausen, A. J., J. R. Asbridge, S. J. Bame, H. E. Gilbert, and I. B. Strong, Vela 3 satellite observations of solar wind ions: A preliminary report, J. Geophys. Res., 72, 87-100, 1967.

Ludwig, G. H., The orbiting geophysical observatories, Space Sci. Rev., 2, 175-218, 1963.

Montgomery, M. D., J. R. Asbridge, and S. J. Bame, Vela 4 plasma observations near the earth's bow shock, J. Geophys. Res., 75, 1217-1231, 1970.

Neugebauer, M., and C. W. Snyder, Mariner 2 observations of the solar wind, 1. Average properties, J. Geophys. Res., 71, 4469-4484, 1966.

Ogilvie, K. W., L. F. Burlaga, and T. D. Wilkerson, Plasma observations on Explorer 34, J. Geophys. Res., 73, 6809-6824, 1968.

Scarf, F. L., J. H. Wolfe, and R. W. Silva, A plasma instability associated with thermal anisotropies in the solar wind, J. Geophys. Res., 72, 993-1005, 1967.

A table of Hermite Polynomials is given in: Magnus, W., and F. Oberhettinger, Formulas and Theorems for the Special Functions of Mathematical Physics, Chelsea Publishing Co., p. 80, 1949.

Two other references were very useful in applying Hermite polynomials to this particular problem:

Margenau, H., and G. M. Murphy, The Mathematics of Physics and Chemistry, D. Van Nostrand, New York, pp. 419-422, 1950.

Whitehead, A. B., R. H. Parker, and E. L. Haines, Use of Transformations in Multiparameter Data Sorting, IEEE, NS-14, 599, 1967.

APPENDIX 1

FARADAY CUP

A scale drawing of the Faraday cup detector is shown on the left side of Fig. 11. The area of the circular aperture is 20.3 cm^2. The structures labeled G, S, and M are ground, suppressor, and modulator grids, respectively. The thick ground grid is actually a solid plate with holes in it. The over-all transparency of the combination of grids was experimentally determined to be 21% for normal incidence, and the relative effective aperture decreases almost linearly with the angle of incidence such that the half-width at half-maximum is 20.3°.

The structure denoted by $C_{1,2,3}$ is actually three separate collectors, each in the shape of a 120° sector. C_4 is a separate collector for particles that arrive at angles greater than $\sim 12^\circ$. The right side of Fig. 11 shows these four collectors as viewed from above, together with a smaller off-center circle that represents an image of the entrance aperture for particles incident from a direction defined by the angles α and β (R is a constant). The sizes of the shaded areas A_1, A_2, A_3, and A_4 are proportional to the currents to collectors 1 through 4, respectively. For observations in the solar wind, A_4 is usually negligible compared with A_1, A_2, and A_3.

Each collector individually and all collectors combined are sequentially connected to an electrometer system whose output is telemetered as a 9-bit number proportional to the current detected, along with one more bit to indicate the sensitivity scale of the electrometer. Measurements

of 1 telemetry unit are equivalent to currents of $(0.512)^{-1} \times 10^{-12}$ and $(0.512)^{-1} \times 10^{-10}$ amp on the high- and low-sensitivity scales, respectively; the instrument switches to the proper scale automatically.

The responses of the Faraday cup and the curved-plate analyzer were experimentally checked with ion, electron, and neutralized ion beams. The following set of equations (relating the ratios $L = A_3/A_1$ and $M = A_2/A_1$ to the angles α and β) was derived from the calibration measurements, using both 1- and 5-keV argon ion beams with energy spreads of $\sim$ 3 eV full width at half-maximum:

$$\beta(\text{deg}) = (10.2 - 10.2\ L) \text{ if } L \geq 0.5$$

$$= (14.7 - 19.2\ L) \text{ if } 0.25 \leq L \leq 0.5$$

$$= (18.9 - 36.0\ L) \text{ if } L \leq 0.25$$

$$\alpha(\text{deg}) = \frac{(1-M)(1+2L)}{(1-L)(1+M+L)} \times 60$$

Figure 12 illustrates the accuracy to which α and β can be determined for a particular example in which $A_1 + A_2 + A_3 = 40$ telemetry units, which is equivalent to a fairly weak solar wind with a total charge flux of 1.35×10^8 charges $cm^{-2} sec^{-1}$. The distance between points in this figure indicates the uncertainty in α and β arising from the digitization of the collector currents.

The angle α is measured counterclockwise (as viewed from the sun) from the center of collector 1. The orientation of the Faraday cup is such that the angles θ_o and φ_o used in analysis of the curved plate analyzer data are given by:

$$|\theta_o| = \beta|\sin(\alpha + 45^\circ)|$$

$$\varphi_o = \beta \cos(\alpha + 45^\circ)$$

The sign of θ_o is not important due to the symmetry of the curved plate analyzer.

APPENDIX 2

FURTHER DETAILS OF THE CURVED PLATE ANALYZER

The electrometer connected to the curved plate analyzer has three sensitivity scales with automatic switching between scales. The input current to the electrometer is directly proportional to the output voltage, which is digitized as a 9-bit number, along with 1 bit for polarity and 2 bits for scale indication. Table 2 gives the sensitivity, range, and rise time of each of the three electrometer scales. The data presented in this report are on the middle and the most sensitive scales. Owing to the electronic transients generated when a scale change is made, the first current measurement made after a switch from the most sensitive to the middle scale and the current measurements in the first m channels made after a switch from the middle to the most sensitive scale have been eliminated before analysis of the spectra, where m = 1, 4 and 8 for spacecraft data rates of 1, 8, and 64 kbit/sec, respectively. At 64 kbit/sec, when the peak of the proton spectrum is on the middle scale, which it often is, the elimination of eight channels' worth of data upon switching back to the most sensitive scale usually results in the elimination of most of the α-particle spectral peak.

A correction must also be made to the zero-current level of the measured spectra to account for an anomalous "photodip" caused by photoelectrons entering the electrometer system through an exposed slit in the electronics' cover plate. This photodip is about 20 channels wide and reaches a peak negative current of between 2 and 8 $\times 10^{-12}$ amp at or near

channel 72 (E/Q = 348 volts). It varies somewhat in both amplitude and channel. A few examples are shown in Fig. 13. Fortunately, the photodip can usually be separated from the positive peaks of the solar wind ions; the separation process is aided by observations made when little or no positive-ion flux enters the analyzer, as often occurs in the magnetosheath and magnetosphere.

The positive-ion data reported here consist of "narrow-fine" spectra for which the instrument measured the currents in only the 32 consecutive channels surrounding the channel with the largest current, as determined by the previous spectrum. It is also possible to sample all 128 channels consecutively ("wide-fine" spectra) or to sample only every fourth channel ("wide-coarse" spectra). Compared with the wide-fine mode, the peak-seeking feature of the narrow-fine mode of operation allows a fourfold increase in the rate of obtaining spectra, with no loss of energy resolution. Unfortunately, the instrument will choose the anomalous photodip as the "peak" if it has greater magnitude (sign is not examined) than the true ion peak. Thus, narrow-fine spectra occasionally miss the solar wind peak entirely.

Furthermore, wide-fine, wide-coarse, or narrow-fine electron spectra can be obtained by reversing the polarity of the deflection voltage and grounding the suppressor grid when low-energy electrons are detected. The methods described in this paper could be applied to electron data, but other methods (which will be described in a separate report) are also available for cases when it can be assumed that the electron distribution function is isotropic in the satellite frame of reference.

APPENDIX 3. LISTING OF TAB (I, J, L)

ξ	Φ_0	$T(U_I/U_0, \Phi_0, \xi)$ for $I = 1, 16$								
1.2	-10.	.00344	.00470	.00631	.00832	.01072	.01347	.01647	.01953	1
1.2	-10.	.02237	.02468	.02613	.02642	.02542	.02315	.01985	.01594	2
1.2	-8.	.00393	.00539	.00727	.00962	.01244	.01570	.01926	.02282	1
1.2	-8.	.02636	.02919	.03102	.03148	.03040	.02778	.02390	.01926	2
1.2	-6.	.00437	.00602	.00814	.01080	.01401	.01773	.02181	.02603	1
1.2	-6.	.03002	.03334	.03551	.03614	.03497	.03203	.02762	.02230	2
1.2	-4.	.00474	.00653	.00886	.01177	.01530	.01940	.02392	.02960	1
1.2	-4.	.03304	.03675	.03921	.03995	.03871	.03549	.03063	.02475	2
1.2	-2.	.00500	.00690	.00937	.01246	.01622	.02058	.02540	.03039	1
1.2	-2.	.03513	.03910	.04173	.04253	.04121	.03777	.03258	.02631	2
1.2	0.	.00513	.00709	.00963	.01281	.01667	.02116	.02611	.03124	1
1.2	0.	.03610	.04016	.04283	.04361	.04220	.03863	.03327	.02691	2
1.2	2.	.00513	.00709	.00961	.01279	.01663	.02109	.02599	.03105	1
1.2	2.	.03593	.03990	.04236	.04305	.04156	.03794	.03258	.02617	2
1.2	4.	.00499	.00689	.00933	.01239	.01608	.02036	.02504	.02985	1
1.2	4.	.03436	.03806	.04040	.04092	.03936	.03580	.03061	.02448	2
1.2	6.	.00473	.00651	.00880	.01166	.01505	.01905	.02336	.02775	1
1.2	6.	.03183	.03512	.03714	.03745	.03586	.03244	.02759	.02193	2
1.2	8.	.00436	.00598	.00806	.01064	.01373	.01726	.02109	.02495	1
1.2	8.	.02848	.03129	.03289	.03298	.03140	.02924	.02385	.01882	2
1.2	10.	.00391	.00535	.00718	.00943	.01211	.01516	.01842	.02168	1
1.2	10.	.02462	.02687	.02807	.02796	.02644	.02359	.01977	.01547	2
1.4	-10.	.00310	.00421	.00696	.00997	.01378	.01835	.02339	.02842	1
1.4	-10.	.03277	.03564	.03635	.03455	.03039	.02458	.01811	.01207	2
1.4	-8.	.00381	.00581	.00863	.01242	.01726	.02308	.02957	.03610	1
1.4	-8.	.04179	.04565	.04674	.04461	.03938	.03194	.02362	.01579	2
1.4	-6.	.00449	.00688	.01025	.01481	.02066	.02772	.03562	.04362	1
1.4	-6.	.05066	.05548	.05695	.05445	.04817	.03914	.02897	.01938	2

1.4	-4.	.00509	.00782	.01167	.01690	.02363	.03178	.04091	.05018	1
1.4	-4.	.05836	.06397	.06572	.06286	.05562	.04518	.03342	.02239	2
1.4	-2.	.00554	.00852	.01274	.01847	.02584	.03477	.04478	.05494	1
1.4	-2.	.06387	.06998	.07193	.06864	.06063	.04915	.03627	.02417	2
1.4	0.	.00579	.00991	.01332	.01950	.02700	.03631	.04672	.05724	1
1.4	0.	.06644	.07265	.07439	.07088	.06239	.05038	.03702	.02455	2
1.4	2.	.00582	.00894	.01334	.01931	.02697	.03619	.04645	.05675	1
1.4	2.	.06567	.07156	.07298	.06921	.06062	.04867	.03555	.02342	2
1.4	4.	.00561	.00860	.01281	.01848	.02573	.03441	.04400	.05354	1
1.4	4.	.06167	.06685	.06780	.06390	.05559	.04431	.03211	.02097	2
1.4	6.	.00519	.00793	.01178	.01692	.02346	.03122	.03972	.04805	1
1.4	6.	.05500	.05924	.05963	.05578	.04812	.03800	.02726	.01762	2
1.4	8.	.00462	.00702	.01037	.01482	.02042	.02701	.03414	.04101	1
1.4	8.	.04659	.04976	.04966	.04600	.03928	.03069	.02176	.01388	2
1.4	10.	.00394	.00595	.00874	.01241	.01697	.02228	.02794	.03328	1
1.4	10.	.03746	.03962	.03913	.03584	.03025	.02333	.01632	.01026	2
1.6	-10.	.00182	.00327	.00562	.00921	.01431	.02094	.02868	.03648	1
1.6	-10.	.04277	.04584	.04449	.03876	.02958	.02036	.01200	.00605	2
1.6	-8.	.00248	.00448	.00774	.01277	.01996	.02936	.04039	.05161	1
1.6	-8.	.06076	.06534	.06364	.05559	.04309	.02933	.01731	.00875	2
1.6	-6.	.00318	.00578	.01004	.01661	.02605	.03844	.05304	.06790	1
1.6	-6.	.08008	.08624	.08406	.07343	.05692	.03871	.02282	.01152	2
1.6	-4.	.00386	.00702	.01222	.02027	.03184	.04704	.06494	.08316	1
1.6	-4.	.09802	.10544	.10261	.08943	.06914	.04686	.02752	.01383	2
1.6	-2.	.00441	.00803	.01399	.02322	.03645	.05380	.07418	.09480	1
1.6	-2.	.11146	.11951	.11582	.10048	.07725	.05205	.03037	.01515	2
1.6	0.	.00476	.00865	.01506	.02495	.03908	.05754	.07909	.10060	1
1.6	0.	.11780	.12560	.12090	.10420	.07947	.05307	.03067	.01515	2

1.6	2.	.00484	.00878	.01524	.02515	.03926	.05753	.07863	.09949	1
1.6	2.	.11561	.12235	.11682	.09970	.07525	.04969	.02837	.01383	2
1.6	4.	.00463	.00838	.01448	.02379	.03691	.05377	.07296	.09158	1
1.6	4.	.10546	.11051	.10438	.08802	.06558	.04271	.02402	.01152	2
1.6	6.	.00419	.00753	.01293	.02110	.03249	.04694	.06311	.07843	1
1.6	6.	.08935	.09249	.08622	.07166	.05258	.03367	.01860	.00875	2
1.6	8.	.00356	.00636	.01094	.01753	.02675	.03825	.05086	.06246	1
1.6	8.	.07023	.07166	.06578	.05377	.03874	.02433	.01316	.00606	2
1.6	10.	.00285	.00505	.00852	.01364	.02058	.02907	.03816	.04620	1
1.6	10.	.05116	.05136	.04630	.03713	.02620	.01609	.00850	.00382	2
1.8	-10.	.00055	.00131	.00287	.00586	.01101	.01886	.02915	.04023	1
1.8	-10.	.04899	.05196	.04736	.03654	.02350	.01239	.00524	.00174	2
1.8	-8.	.00088	.00208	.00460	.00944	.01782	.03063	.04750	.06569	1
1.8	-8.	.08009	.08500	.07746	.05973	.03837	.02018	.00853	.00284	2
1.8	-6.	.00128	.00304	.00674	.01386	.02621	.04509	.06992	.09658	1
1.8	-6.	.11752	.12437	.11290	.08670	.05541	.02999	.01219	.00403	2
1.8	-4.	.00171	.00407	.00904	.01859	.03511	.06028	.09318	.12920	1
1.8	-4.	.15517	.16319	.14710	.11205	.07099	.03690	.01532	.00503	2
1.8	-2.	.00211	.00502	.01112	.02281	.04291	.07333	.11767	.15392	1
1.8	-2.	.18476	.19249	.17167	.12924	.08089	.04138	.01701	.00550	2
1.8	0.	.00240	.00569	.01256	.02563	.04791	.08127	.12380	.16740	1
1.8	0.	.19870	.20440	.17980	.13330	.08210	.04130	.01668	.00530	2
1.8	2.	.00252	.00594	.01302	.02638	.04885	.08211	.12365	.16508	1
1.8	2.	.19315	.19557	.16908	.12306	.07427	.03658	.01445	.00449	2
1.8	4.	.00244	.00570	.01239	.02487	.04559	.07561	.11228	.14760	1
1.8	4.	.16971	.16858	.14272	.10155	.05983	.02873	.01105	.00334	2
1.8	6.	.00217	.00502	.01081	.02144	.03879	.06339	.09258	.11948	1
1.8	6.	.13459	.13071	.10799	.07483	.04284	.01996	.00743	.00217	2

1.8	9.	.00177	.00406	.00962	.01686	.03004	.04825	.06914	.08734	1
1.8	8.	.09612	.09097	.07306	.04910	.02720	.01223	.00439	.00123	2
1.9	10.	.00132	.00299	.00627	.01206	.02111	.03324	.04659	.05746	1
1.9	10.	.06159	.05662	.04406	.02960	.01526	.00659	.00226	.00061	2
2.0	-10.	.00000	.00023	.00075	.00219	.00559	.01239	.02346	.03732	1
2.0	-10.	.04900	.05208	.04389	.02865	.01413	.00511	.00132	.00023	2
2.0	-8.	.00000	.00046	.00150	.00435	.01110	.02456	.04633	.07333	1
2.0	-8.	.09570	.10100	.08445	.05469	.02675	.00982	.00247	.00044	2
2.0	-6.	.00000	.00080	.00260	.00755	.01921	.04225	.07909	.12399	1
2.0	-6.	.15999	.16678	.13756	.08788	.04243	.01508	.00383	.00067	2
2.0	-4.	.00000	.00123	.00400	.01155	.02915	.06346	.11741	.18159	1
2.0	-4.	.23073	.23643	.19156	.12012	.05695	.01988	.00497	.00086	2
2.0	-2.	.00000	.00170	.00547	.01563	.03900	.08379	.15262	.23195	1
2.0	-2.	.28900	.28993	.22972	.14077	.06521	.02226	.00545	.00093	2
2.0	0.	.00000	.00209	.00668	.01884	.04632	.09782	.17480	.25990	1
2.0	0.	.31620	.30920	.23950	.14210	.06395	.02123	.00506	.00084	2
2.0	2.	.00000	.00232	.00731	.02030	.04901	.10137	.17693	.25639	1
2.0	2.	.30325	.28761	.21463	.12357	.05370	.01721	.00396	.00063	2
2.0	4.	.00000	.00232	.00718	.01956	.04623	.09333	.15849	.22274	1
2.0	4.	.25480	.23302	.16726	.09238	.03845	.01178	.00259	.00040	2
2.0	6.	.00060	.00207	.00629	.01678	.03869	.07600	.12511	.16982	1
2.0	6.	.18690	.16383	.11228	.05903	.02331	.00676	.00141	.00000	2
2.0	8.	.00049	.00163	.00487	.01270	.02851	.05431	.08638	.11277	1
2.0	8.	.11880	.09922	.06949	.03200	.01188	.00323	.00063	.00000	2
2.0	10.	.00034	.00113	.00330	.00839	.01828	.03367	.05157	.06451	1
2.0	10.	.06477	.05127	.03141	.01460	.00505	.00127	.00023	.00000	2
2.2	-10.	.00000	.00000	.00000	.00038	.00158	.00530	.01400	.02837	1
2.2	-10.	.04289	.04696	.03597	.01858	.00621	.00128	.00016	.00000	2

2.2	-8.	.00000	.00000	.00000	.00102	.00419	.01382	.03578	.07086	1
2.2	-8.	.10459	.11176	.08368	.04233	.01390	.00283	.00034	.00000	2
2.2	-6.	.00000	.00000	.00045	.00225	.00910	.02938	.07408	.14246	1
2.2	-6.	.20370	.21072	.15283	.07511	.02406	.00481	.00057	.00000	2
2.2	-4.	.00000	.00000	.00085	.00414	.01635	.05157	.12612	.23948	1
2.2	-4.	.32330	.33196	.22501	.10683	.03321	.00648	.00075	.00000	2
2.2	-2.	.00000	.00000	.00135	.00645	.02485	.07589	.17947	.32144	1
2.2	-2.	.42579	.40682	.27283	.12459	.03741	.00709	.00081	.00000	2
2.2	0.	.00000	.00000	.00186	.00864	.03231	.09532	.21700	.37290	1
2.2	0.	.47260	.43110	.27590	.12040	.03463	.00632	.00070	.00000	2
2.2	2.	.00000	.00000	.00226	.01015	.03664	.10382	.22615	.37034	1
2.2	2.	.44566	.38495	.23281	.09592	.02608	.00451	.00047	.00000	2
2.2	4.	.00000	.00000	.00242	.01052	.03643	.09861	.20399	.31543	1
2.2	4.	.35670	.28914	.16237	.05213	.01566	.00251	.00000	.00000	2
2.2	6.	.00000	.00000	.00227	.00947	.03140	.08074	.15754	.22809	1
2.2	6.	.23966	.17861	.09224	.03217	.00736	.00107	.00000	.00000	2
2.2	8.	.00000	.00036	.00180	.00721	.02281	.05556	.10179	.13706	1
2.2	8.	.13259	.09007	.04199	.01310	.00266	.00034	.00000	.00000	2
2.2	10.	.00000	.00024	.00117	.00449	.01353	.03113	.05338	.06656	1
2.2	10.	.05894	.03619	.01506	.00414	.00073	.00008	.00000	.00000	2
2.4	-10.	.00000	.00000	.00000	.00000	.00019	.00122	.00555	.01688	1
2.4	-10.	.03282	.03987	.02652	.00980	.00193	.00016	.00000	.00000	2
2.4	-8.	.00000	.00000	.00000	.00000	.00076	.00472	.02025	.05786	1
2.4	-8.	.10588	.11944	.07688	.02726	.00494	.00042	.00000	.00000	2
2.4	-6.	.00000	.00000	.00000	.00000	.00234	.01366	.05461	.14488	1
2.4	-6.	.24592	.25615	.15613	.05261	.00918	.00077	.00000	.00000	2
2.4	-4.	.00000	.00000	.00000	.00070	.00548	.03005	.11192	.27979	1
2.4	-4.	.43063	.41553	.23681	.07570	.01274	.00104	.00000	.00000	2

2.4	-2.	.00000	.00000	.00000	.00134	.00996	.05146	.17914	.40851	1
2.4	-2.	.59293	.53113	.28327	.09590	.01393	.00112	.00000	.00000	2
2.4	0.	.00000	.00000	.00000	.00208	.01466	.07134	.23240	.49320	1
2.4	0.	.66410	.55190	.27420	.07807	.01201	.00093	.00000	.00000	2
2.4	2.	.00000	.00000	.00000	.00280	.01855	.08420	.25439	.49797	1
2.4	2.	.61560	.46784	.21213	.05513	.00778	.00055	.00000	.00000	2
2.4	4.	.00000	.00000	.00000	.00337	.02077	.08680	.23917	.42316	1
2.4	4.	.46860	.31637	.12642	.02880	.00356	.00000	.00000	.00000	2
2.4	6.	.00000	.00000	.00042	.00350	.01992	.07596	.18823	.29492	1
2.4	6.	.28484	.16535	.05604	.01071	.00110	.00000	.00000	.00000	2
2.4	8.	.00000	.00000	.00037	.00289	.01521	.05277	.11687	.16036	1
2.4	8.	.13268	.06458	.01799	.00278	.00023	.00000	.00000	.00000	2
2.4	10.	.00000	.00000	.00024	.00176	.00856	.02702	.05342	.06395	1
2.4	10.	.04504	.01815	.00408	.00050	.00003	.00000	.00000	.00000	2
2.6	-10.	.00000	.00000	.00000	.00000	.00000	.00011	.00121	.00717	1
2.6	-10.	.02147	.02996	.01777	.00402	.00031	.00001	.00000	.00000	2
2.6	-8.	.00000	.00000	.00000	.00000	.00000	.00077	.00737	.03797	1
2.6	-8.	.09959	.12348	.06637	.01397	.00102	.00000	.00000	.00000	2
2.6	-6.	.00000	.00000	.00000	.00000	.00025	.00361	.02918	.12726	1
2.6	-6.	.28425	.30570	.14669	.02853	.00200	.00000	.00000	.00000	2
2.6	-4.	.00000	.00000	.00000	.00000	.00091	.01141	.07883	.29047	1
2.6	-4.	.54979	.51192	.22090	.04040	.00277	.00000	.00000	.00000	2
2.6	-2.	.00000	.00000	.00000	.00000	.00221	.02475	.14973	.47742	1
2.6	-2.	.78361	.64521	.25486	.04440	.00298	.00000	.00000	.00000	2
2.6	0.	.00000	.00000	.00000	.00000	.00385	.03914	.21230	.60240	1
2.6	0.	.88000	.65050	.23420	.03788	.00241	.00000	.00000	.00000	2
2.6	2.	.00000	.00000	.00000	.00000	.00563	.05132	.24860	.62575	1
2.6	2.	.90501	.51928	.16170	.02263	.00126	.00000	.00000	.00000	2

2.6	4.	.00000	.00000	.00000	.00052	.00768	.06111	.25462	.54325	1
2.6	4.	.58264	.30634	.07593	.00833	.00037	.00000	.00000	.00000	2
2.6	6.	.00000	.00000	.00000	.00070	.00911	.06219	.21622	.37291	1
2.6	6.	.31311	.12503	.02282	.00180	.00000	.00000	.00000	.00000	2
2.6	8.	.00000	.00000	.00000	.00070	.00800	.04664	.13384	.18281	1
2.6	9.	.11604	.03347	.00424	.00022	.00000	.00000	.00000	.00000	2
2.6	10.	.00000	.00000	.00002	.00045	.00445	.02238	.05284	.05685	1
2.6	10.	.02702	.00553	.00047	.00002	.00000	.00000	.00000	.00000	2
2.8	-10.	.00000	.00000	.00000	.00000	.00000	.00000	.00010	.00183	1
2.8	-10.	.01132	.02165	.01085	.00117	.00002	.00000	.00000	.00000	2
2.8	-8.	.0	.0	.0	.0	.0	.00004	.00139	.01817	1
2.8	-8.	.08557	.12880	.05378	.00520	.00009	.00000	.00000	.00000	2
2.8	-6.	.00000	.00000	.00000	.00000	.00000	.00042	.00990	.09236	1
2.8	-6.	.31540	.36230	.12460	.01082	.00019	.00000	.00000	.00000	2
2.8	-4.	.00000	.00000	.00000	.00000	.00000	.00243	.04151	.27410	1
2.8	-4.	.57640	.60300	.18020	.01506	.00027	.00000	.00000	.00000	2
2.8	-2.	.00000	.00000	.00000	.00000	.00000	.00793	.10410	.51900	1
2.8	-2.	.98760	.73140	.20030	.01646	.00030	.00000	.00000	.00000	2
2.8	0.	.00000	.00000	.00000	.00000	.00051	.01514	.16640	.68970	1
2.8	0.	1.10200	.71350	.17550	.01330	.00023	.00000	.00000	.00000	2
2.8	2.	.00000	.00000	.00000	.00000	.00088	.02232	.20980	.73770	1
2.8	2.	1.00400	.53320	.10350	.00621	.00000	.00000	.00000	.00000	2
2.8	4.	.00000	.00000	.00000	.00000	.00157	.03251	.24390	.67130	1
2.8	4.	.68980	.25890	.03293	.00126	.00000	.00000	.00000	.00000	2
2.8	6.	.00000	.00000	.00000	.00000	.00256	.04213	.23840	.46400	1
2.8	6.	.31490	.07303	.00532	.00011	.00000	.00000	.00000	.00000	2
2.8	8.	.00000	.00000	.00000	.00008	.00296	.03734	.15400	.20260	1
2.8	8.	.08942	.01091	.00042	.00000	.00000	.00000	.00000	.00000	2

2.8	10.	.00000	.00000	.00000	.00006	.00185	.01784	.05241	.04510	1
2.8	10.	.01127	.00080	.00002	.00000	.00000	.00000	.00000	.00000	2
3.0	-10.	.00000	.00000	.00000	.00000	.00000	.00000	.00000	.00021	1
3.0	-10.	.00436	.01486	.00596	.00020	.00000	.00000	.00000	.00000	2
3.0	-8.	.00000	.00000	.00000	.00000	.00000	.00000	.00010	.00535	1
3.0	-8.	.06419	.13550	.04025	.00118	.00000	.00000	.00000	.00000	2
3.0	-6.	.00000	.00000	.00000	.00000	.00000	.00000	.00175	.05190	1
3.0	-6.	.33380	.42750	.09271	.00245	.00000	.00000	.00000	.00000	2
3.0	-4.	.00000	.00000	.00000	.00000	.00000	.00022	.01481	.22720	1
3.0	-4.	.80320	.67740	.12800	.00348	.00000	.00000	.00000	.00000	2
3.0	-2.	.00000	.00000	.00000	.00000	.00000	.00152	.05976	.52980	1
3.0	-2.	1.19200	.78260	.14100	.00391	.00000	.00000	.00000	.00000	2
3.0	0.	.00000	.00000	.00000	.00000	.00000	.00398	.11420	.73550	1
3.0	0.	1.30800	.74420	.11870	.00304	.00000	.00000	.00000	.00000	2
3.0	2.	.00000	.00000	.00000	.00000	.00000	.00654	.15440	.82150	1
3.0	2.	1.202	.51610	.05509	.00098	.00000	.00000	.00000	.00000	2
3.0	4.	.00000	.00000	.00000	.00000	.00014	.01226	.20860	.79950	1
3.0	4.	.78260	.18740	.00907	.00007	.00000	.00000	.00000	.00000	2
3.0	6.	.00000	.00000	.00000	.00000	.00034	.02176	.24950	.56750	1
3.0	6.	.28530	.03033	.00054	.00000	.00000	.00000	.00000	.00000	2
3.0	8.	.00000	.00000	.00000	.00000	.00064	.02558	.17760	.21520	1
3.0	8.	.04775	.00178	.00001	.00000	.00000	.00000	.00000	.00000	2
3.0	10.	.00000	.00000	.00000	.00000	.00053	.01375	.05281	.02978	1
3.0	10.	.00266	.00004	.00000	.00000	.00000	.00000	.00000	.00000	2
3.0	10.	.00266	.00004	.00000	.00000	.00000	.00000	.00000	.00000	2

APPENDIX 4. FORTRAN SUBROUTINES

```
@FOR,IS FIT,FIT
      SUBROUTINE FIT(UPMAG,VEL,TEMP,DEN,NUTS)
      COMMON /MOMENT/ IGO,ISTOP,TA(16,10),J,MAXT(10)
      COMMON /MAXCH/MAXCH
      COMMON /TABLE/ TAB(16,11,10)
      COMMON /IPART/ IPART
     1       /ANGO/ THETA,PHI,TFLX,CONE,CLOCK
     1       /NOP/ NCHAN
     1       /ICHAN/ ICHAN(20)
      DIMENSION T3(10),T4(10)
      DIMENSION VA(16),TH(16),XSAVE(10)
      DIMENSION  UPMAG(1)
      DIMENSION           VAR(17),          TZ(10),TF(10),TS(10)
      JM=IFIX(PHI+12.)/2-1
      IF(JM.LT.1) JM=1
      IF(JM.GT.8) JM=8
      DO 32 L=1,10
      TMAX=0.
      DO 31 I=1,16
      DO 30 J=1,11
   30 VAR(J)=TAB(I,J,L)
      CALL INTRP((PHI+12.)/2.,VAR,TA(I,L),JM,4)
      IF(TA(I,L).LT.TMAX) GO TO 31
      TMAX=TA(I,L)
      MAXT(L)=I
   31 CONTINUE
   32 CONTINUE
      EMAX=0.
```

UPMAG (I) = $d(I)$ = current meas.

IPART = 1 for protons
= 2 for alphas

THETA = θ_0

PHI = φ_0

NCHAN = number of points in spectrum

ICHAN (I) = channel numbers

INTRP is an interpolation subroutine

```
      DO 34 I=1,NCHAN
      IF(UPMAG(I).LE.EMAX) GO TO 34
      EMAX=UPMAG(I)
      MAXE=I
      MAXCH=ICHAN(I)
   34 CONTINUE
      EXPK=(UPMAG(MAXE+1)-UPMAG(MAXE-1))/2./(2.*EMAX-UPMAG(MAXE+1)-UPMAG
     1(MAXE-1))
      DO 38 L=1,10
      LP=MAXT(L)
      TXPK=(TA(LP+1,L)-TA(LP-1,L))/2./(2.*TA(LP,L)-TA(LP+1,L)-TA(LP-1,L)
     1)
      DO 36 I=1,16
   36 VA(I)=TA(I,L)
      DO 37 M=1,NCHAN
      X=TXPK-EXPK+FLOAT(LP+M-MAXE)
      IF(M.EQ.MAXE) XSAVE(L)=X
      IGO=X-1.
      IF(IGO.LT.1) IGO=1
      IF(IGO.GT.13) IGO=13
      CALL INTRP(X,VA,TH(M),IGO,4)
      IF(TH(M).LT.0.) TH(M)=0.
   37 CONTINUE
      TZ(L)=SMP(TH,1,NCHAN)
      TF(L)=FMOE(1,TH)/TZ(L)
      TS(L)=FMOE(2,TH)/TZ(L)-TF(L)**2
      IF(TS(L).LE.0.) GO TO 43
      T3(L)=(TS(L)**(-1.5))*(FMOE(3,TH)/TZ(L)-3.*TF(L)*TS(L)-TF(L)**3)
```

EMAX = largest $\mathcal{A}(I)$

MAXE = I of largest $\mathcal{A}(I)$ = max

MAXCH = channel number of largest $\mathcal{A}(I)$

EXPK = $\chi(\text{peak})^m$

TXPK = $\chi(\text{peak}, L)^t$

$X = \chi_i$

$TZ(L) = C_0^t(L)$

$TF(L) = C_1^t(L)$

$TS(L) = C_2^t(L)$

$T3(L) = C_3^t(L)$

```
      T4(L)=(TS(L)**(-2))*(FMOE(4,TH)/TZ(L)-4.*TF(L)*(TS(L)**(1.5))*T3(L
     1)-6.*TF(L)**2*TS(L)-TF(L)**4)-3.
      WRITE(6,40) L,TZ(L),TF(L),TS(L),T3(L),T4(L)
   40 FORMAT(I4,5E10.3,I4)
   39 CONTINUE
      EZ=SMP(UPMAG,1,NCHAN)
      EF=FMOE(1,UPMAG)/EZ
      ES=FMOE(2,UPMAG)/EZ-EF*EF
      IF(ES.GT.0.)GO TO 44
      WRITE(6,144)
  144 FORMAT(13H NEGATIVE ES.)
      NUTS=2
      RETURN
   44 E3=ES**(-1.5)*(FMOE(3,UPMAG)/EZ-3.*EF*ES-EF**3)
      E4=ES**(-2)*(FMOE(4,UPMAG)/EZ-4.*EF*(ES**1.5)*E3-6.*(EF**2)*ES-EF*
     1*4)-3.
      J=0
      WRITE(6,40)J,EZ,EF,ES,E3,E4
      KNT=0
      DO 52 J=1,9
      IF(TS(J).GE.ES.AND.TS(J+1).LT.ES) GO TO 51
      GO TO 52
   51 JZ=J
      KNT=KNT+1
   52 CONTINUE
      IF(KNT.EQ.1) GO TO 60
      IF(KNT.EQ.0) WRITE(6,53)
    3 FORMAT(33H ES NOT WITHIN RANGE OF TS TABLE.)
```

$T4(L) = C_4^t(L)$

$EZ = C_0^m$

$EF = C_1^m$

$ES = C_2^m$

$E3 = C_3^m$

$E4 = C_4^m$

If NUTS = 1, all is O.K.
= 2, couldn't fit spectrum

```
      IF(KNT.GT.1) WRITE(6,54)
   54 FORMAT(23H TS TABLE MULTI-VALUED.)
   55 NUTS =2
      RETURN
   49 WRITE(6,50)
   50 FORMAT(22H NEGATIVE TS(J) VALUE.)
      GO TO 55
   60 IGO=J7
      IF(IGO.GT.7) IGO=7
      YZ=TS(IGO)
      Y1=TS(IGO+1)
      Y2=TS(IGO+2)
      Y3=TS(IGO+3)
      XZ=IGO
      X=(ES-Y1)*(ES-Y2)*(ES-Y3)/(YZ-Y1)/(YZ-Y2)/(YZ-Y3)*XZ
     1 +(ES-YZ)*(ES-Y2)*(ES-Y3)/(Y1-YZ)/(Y1-Y2)/(Y1-Y3)*(XZ+1.)
     2 +(ES-YZ)*(ES-Y1)*(ES-Y3)/(Y2-YZ)/(Y2-Y1)/(Y2-Y3)*(XZ+2.)
     3 +(ES-YZ)*(ES-Y1)*(ES-Y2)/(Y3-YZ)/(Y3-Y1)/(Y3-Y2)*(XZ+3.)
   70 ALROT=0.2*X+1.0                                   ALROT = ξ
      ROT=10.**ALROT
      CALL INTRP(X,TF,F,IGO,4)
      CALL INTRP(X,XSAVE,XUSE,IGO,4)
      CPEAK=FLOAT(MAXCM)+EF-F-XUSE+9.                  CPEAK = x*
      IF(IPART.EQ.2) CPEAK=CPEAK-10.
      VEL=10.**(1.329004+.015052*CPEAK)                VEL = v0
      FACTOR=IPART+2*(IPART-1)
      TEMP=.0803*VEL*VEL*FACTOR/ROT                    TEMP = T
      CALL INTRP(X,TZ,Z,IGO,4)
```

```
      CALL INTRP(X,TS,TSI,IGO,4)
      CALL INTRP(X,T3,T3I,IGO,4)
      CALL INTRP(X,T4,T4I,IGO,4)
      X=ALROT
      THECOR=10.**(THETA*THETA*(5.05006-10.6985*X+8.62214*X**2-1.50611*
     1X**3)/1000.)
      DEN=1.080*EZ/FLOAT(IPART)/Z/VEL*THECOR
      NUTS=1
      J=99
      WRITE(6,40) J,Z,F,TSI,T3I,T4I
      ESKEW=E3-T3I
      SKURT=E4-T4I
      SUME=0.
      SUMC=0.
      COEF=E2/SQRT(6.283*ES)
      WRITE(6,100)
  100 FORMAT(5H CHAN,5X,5HUPMAG,6X,4HCURM,6X,4HCURT)
      DO 105 I=1,NCHAN
      X=(FLOAT(ICHAN(I)-MAXCH)-EF)/SQRT(ES)
      FE=EXP(-0.5*X*X)
      SKEW=X**3-3.*X
      FKURT=X**4-6.*X*X+3.
      CURM=COEF*FE*(1.+E3*SKEW/6.+E4*FKURT/24.)
      SUME=SUME+ (CURM-UPMAG(I))**2
      SUMC=SUMC+UPMAG(I)*UPMAG(I)
      X=(FLOAT(ICHAN(I)-MAXCH)- F)/SQRT(ES)
      FE=EXP(-0.5*X*X)
      SKEW=X**3-3.*X
```

DEN = density = n_p or n_α

CURM = value of currents corresponding to the C_i^m

CURT = value of currents corresponding to the C_i^t

```
      FKURT=X**4-6.*X*X+3.
      CURT=COEF*FE*(1.+T3I*SKEW/6.+T4I*FKURT/24.)
      WRITE(6,101)ICHAN(I),UPMAG(I),CURM,CURT
  101 FORMAT(I5,3F10.0)
  105 CONTINUE
      ELSQ=SUME/SUMC
      WRITE(6,110) ELSQ,ESKEW,EKURT
  110 FORMAT(3F10.5)
      RETURN
      END
@FOR,IS  FMOE
      FUNCTION FMOE(IUP,UPMAG)
      DIMENSION VAR(17),UPMAG(1)
      COMMON /NOP/ NCHAN  /ICHAN/ ICHAN(20)  /MAXCH/ MAXCH
      DO 1 I=1,NCHAN
    1 VAR(I)=UPMAG(I)*FLOAT((ICHAN(I)-MAXCH)**IUP)
      FMOE=SMP(VAR,1,NCHAN)
      RETURN
      END
@FOR,IS  INTRP,INTRP
      SUBROUTINE INTRP(X,VAR,Y,IGO,KNT)
C
C     INTERPOLATION BY BESSELS FORMULA IV ON PAGE 77 OF SCARBOROUGH.
C     IGO IS INDEX OF FIRST OF 4 VALUES OF VAR TO BE USED.
C     DELTA X = H = 1.
C     INPUT X, GET Y OUT.
C
      DIMENSION VAR(1)
```

ELSQ = variation
= HP error

```
      YM=VAR(IGO)
      YZ=VAR(IGO+1)
      DYM=YZ-YM
      IF(KNT.GT.2) GO TO 3
      U=X-FLOAT(IGO)
      Y=YM+U*DYM
      RETURN
    3 Y1=VAR(IGO+2)
      DYZ=Y1-YZ
      DDYM=DYZ-DYM
      U=X-FLOAT(IGO+1)
      IF(KNT.GT.3) GO TO 4
      Y=YZ+U*(DYM+DYZ)/2.+U*U*DDYM/2.
      RETURN
    4 Y2=VAR(IGO+3)
      DY1=Y2-Y1
      DDYZ=DY1-DYZ
      DDDYM=DDYZ-DDYM
      Y=YZ+U*DYZ+U*(U-1.)*(DDYM+DDYZ)/4.+(U-.5)*U*(U-1.)*DDDYM/6.
      RETURN
      END
@FOR,IS  SMP,SMP
      FUNCTION SMP(Y,M1,M2)
      DIMENSION Y(21)
      IODD=0
      N2=M2
      SUM=0.
      IF(MOD(M2-M1,2).EQ.0) GO TO 1
```

```
      Y(M2+1)=0.
      N2=M2+1
    1 DO 10 I=M1,N2
      IODD=IODD+1
      IF(I.EQ.M1.OR.I.EQ.N2) GO TO 4
      IF(MOD(IODD,2).EQ.0) GO TO 2
      SUM=SUM+2.*Y(I)
      GO TO 10
    2 SUM=SUM+4.*Y(I)
      GO TO 10
    4 SUM=SUM+Y(I)
   10 CONTINUE
      SMP=SUM/3.
      RETURN
      END
```

TABLE 1. RESULTS OF FIT BY LEAST SQUARES AND HERMITE POLYNOMIALS

#		particle	v	T	n	LS error	HP error	eskew	ekurt	Δv/v	ΔT/T	Δn/n	Number of points in spectrum
1	-1.6	proton	373.8	87.9	4.1	.0004	.0071	.01	-.01	.000	.007	.024	8
2	-2.6	proton	395.6	56.9	3.1	.0019	.0047	.00	-.01	-.002	.033	.032	7
3	-2.5	alpha	391.0	411.8	0.4	.0040	.0505	-.12	.20	.003	-.094	.000	7
4	-0.2	proton	385.6	53.1	3.4	.0074	.0841	-.03	.08	-.008	-.250	-.206	5
5	-0.1	alpha	386.3	355.8	0.2	.0042	.0110	.08	.16	-.002	.072	.000	8
6	-4.7	proton	322.4	17.0	2.8	.0015	.0059	.01	-.03	.000	-.065	.036	5
7	-5.2	proton	408.8	189.9	8.9	.0123	.0238	.07	.06	-.001	-.167	-.034	9
8	-0.7	proton	406.2	71.5	3.5	.0120	.0579	.22	-.21	.007	-.110	-.029	5
9	-4.5	proton	417.0	48.7	3.6	.0021	.0058	.02	.02	.002	.142	.083	5
10	-1.3	proton	388.5	42.9	3.4	.0003	.0017	.02	-.03	.001	-.023	.029	6
11	-2.1	proton	404.0	86.4	3.4	.0032	.0147	-.02	-.06	-.006	.150	.176	7
12	-4.7	proton	506.7	36.0	5.7	.0012	.0081	.03	.03	.000	-.067	.070	5
13	-6.0	proton	458.5	51.4	3.2	.0019	.0632	.07	.20	-.001	-.066	.031	5
14	-0.8	proton	580.4	181.7	5.6	.0054	.0326	-.16	.19	-.006	-.228	-.125	4
15	5.1	proton	617.3	67.2	12.5	.0035	.0422	.09	.26	.000	-.155	-.104	5
16	-1.1	proton	515.0	33.2	3.3	.0091	.0217	-.09	.19	.002	-.018	-.091	4
17	0.4	proton	542.6	72.0	1.7	.0105	.0567	-.02	.10	-.004	-.224	-.118	5
18	8.2	proton	544.2	1033.9	10.0	.0085	.0429	-.06	-.03	-.019	-.391	-.039	6
19	2.1	proton	531.2	111.2	3.8	.0026	.0149	-.04	.06	-.001	.089	.026	7
20	1.7	proton	513.0	90.2	2.2	.0025	.0027	-.01	-.08	.001	.004	.000	7
21	3.0	proton	440.4	284.9	3.3	.0093	.0547	.06	.06	.001	-.051	.000	7
22	4.3	proton	589.8	42.9	0.6	.0107	.4510	.01	-.02	.001	-.230	-.200	3
23	5.5	proton	460.9	107.9	10.0	.0035	.0243	-.12	.10	-.002	-.077	-.020	7
24	2.7	proton	437.0	69.4	3.4	.0084	.0116	.09	.19	-.002	.049	.029	7
25	9.2	proton	452.3	122.0	4.7	.0076	.0193	.03	.02	-.000	-.029	-.021	7
26	3.3	proton	439.7	225.2	9.1	.0025	.0241	.07	-.09	.007	-.095	-.099	9
27	1.8	proton	442.4	99.2	4.2	.0068	.0978	.09	.01	.001	.095	.072	4
28	2.6	proton	421.2	37.6	2.3	.0006	.0791	.03	-.04	-.001	-.064	-.044	5
			km/sec	10^3 °K	cm^{-3}								

TABLE 2

CHARACTERISTICS OF CURVED-PLATE ANALYZER ELECTROMETER

Scale	Most Sensitive	Middle	Least Sensitive
Current for Digital output = 1, amp	$\frac{10^{-14}}{0.512}$	$\frac{10^{-12}}{0.512}$	$\frac{10^{-10}}{0.512}$
Current for Digital output = 511, amp	$\frac{5.11}{5.12} \times 10^{-11}$	$\frac{5.11}{5.12} \times 10^{-9}$	$\frac{5.11}{5.12} \times 10^{-7}$
Rise time (10 to 90%) seconds	0.25	0.025	Rate Limited

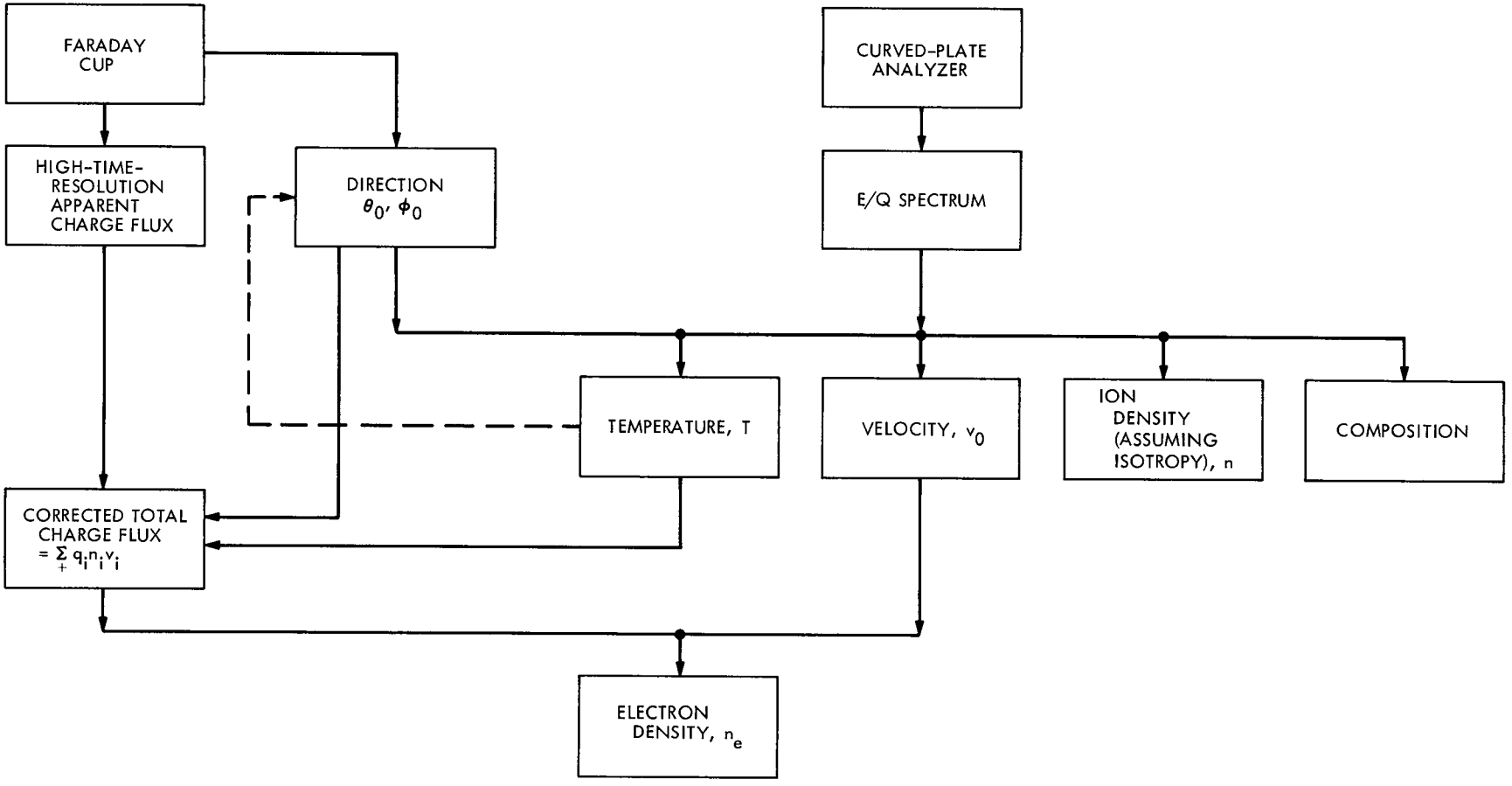

Fig. 1. Logic diagram for the calculation of solar-wind parameters

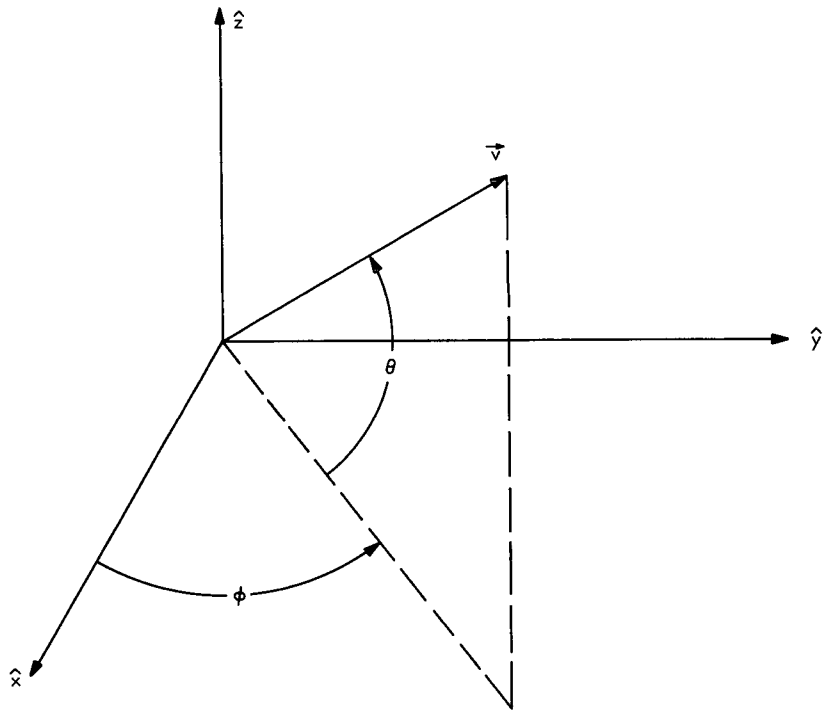

THE SUN IS NOMINALLY IN THE $+\hat{x}$ DIRECTION.
NORMALLY INCIDENT PARTICLES HAVE $\theta = \phi = 0$.
THE xy PLANE IS THE ANALYSIS PLANE.

Fig. 2. Definitions of θ and ϕ

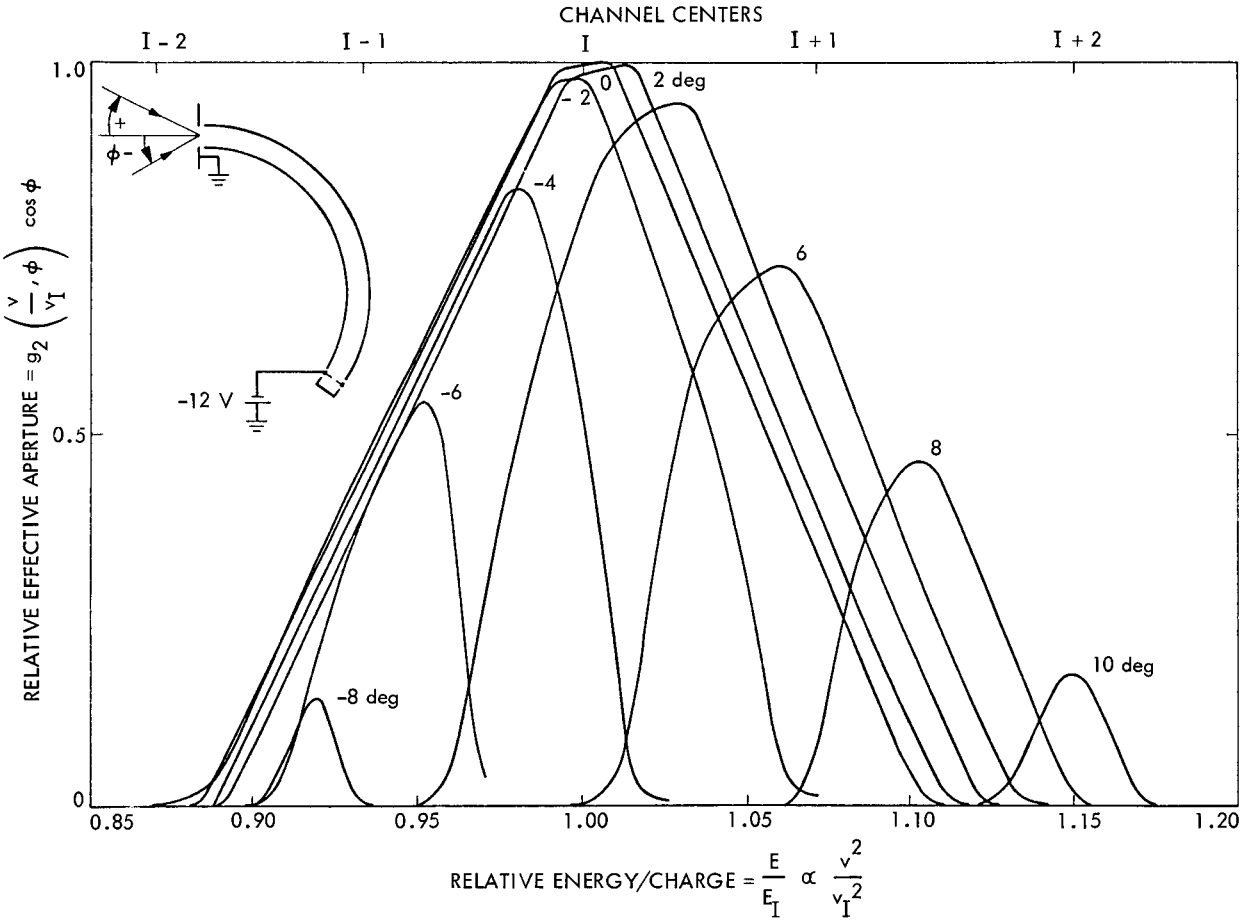

Fig. 3. Relative effective aperture of the curved-plate analyzer

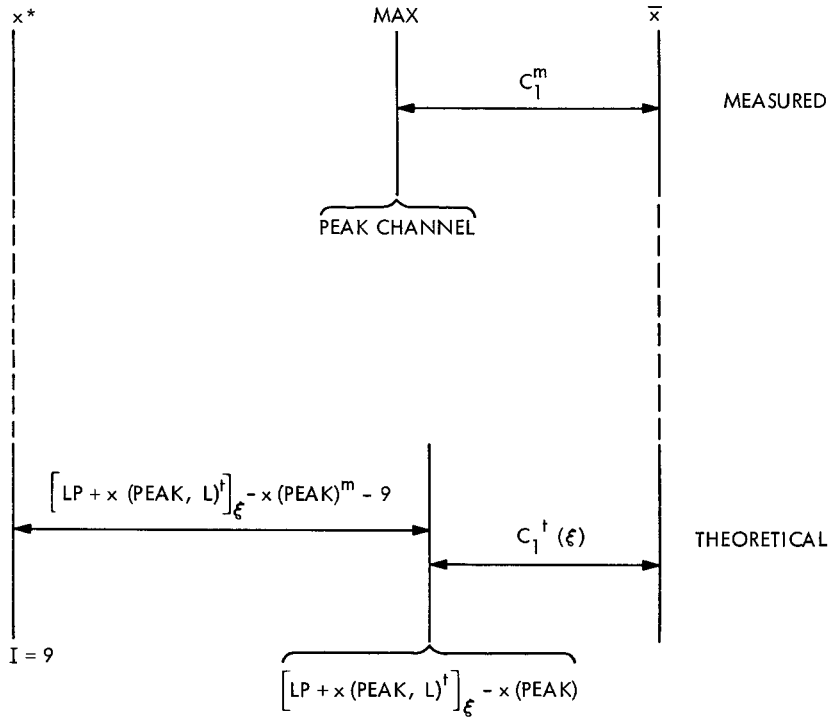

Fig. 4. The relation between x^*, C_1^m, $C_1^t(\xi)$, and the channel number

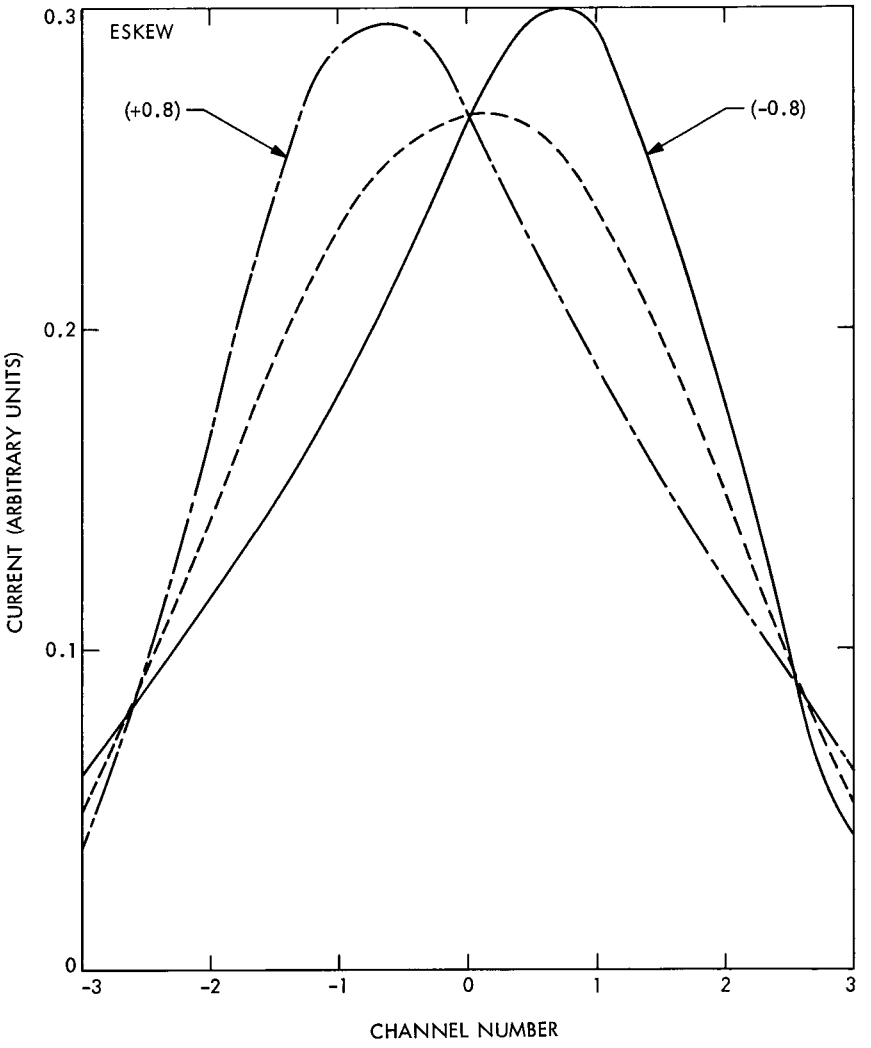

Fig. 5. The effect of a large ESKEW

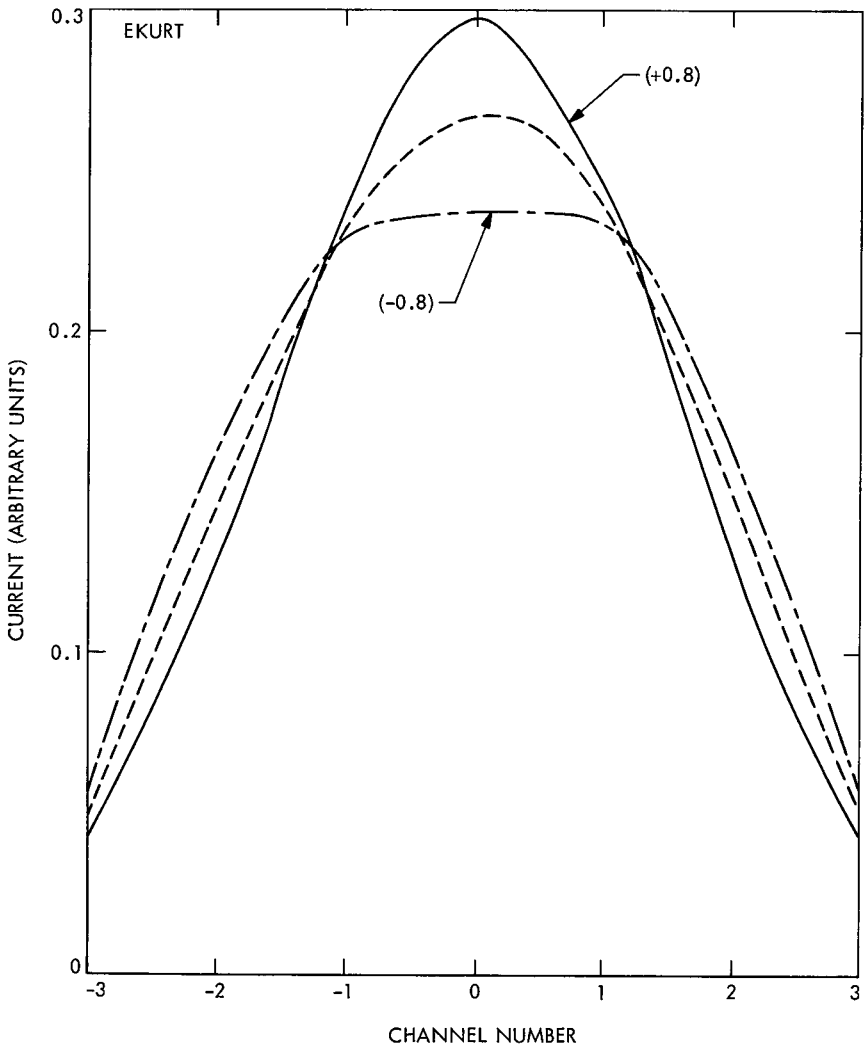

Fig. 6. The effect of a large EKURT

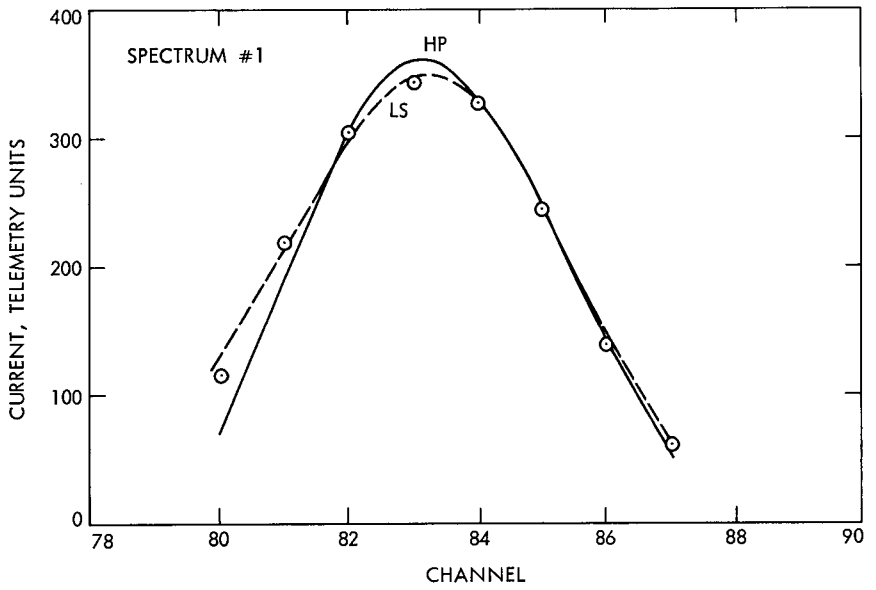

Fig. 7. The fit of spectrum #1

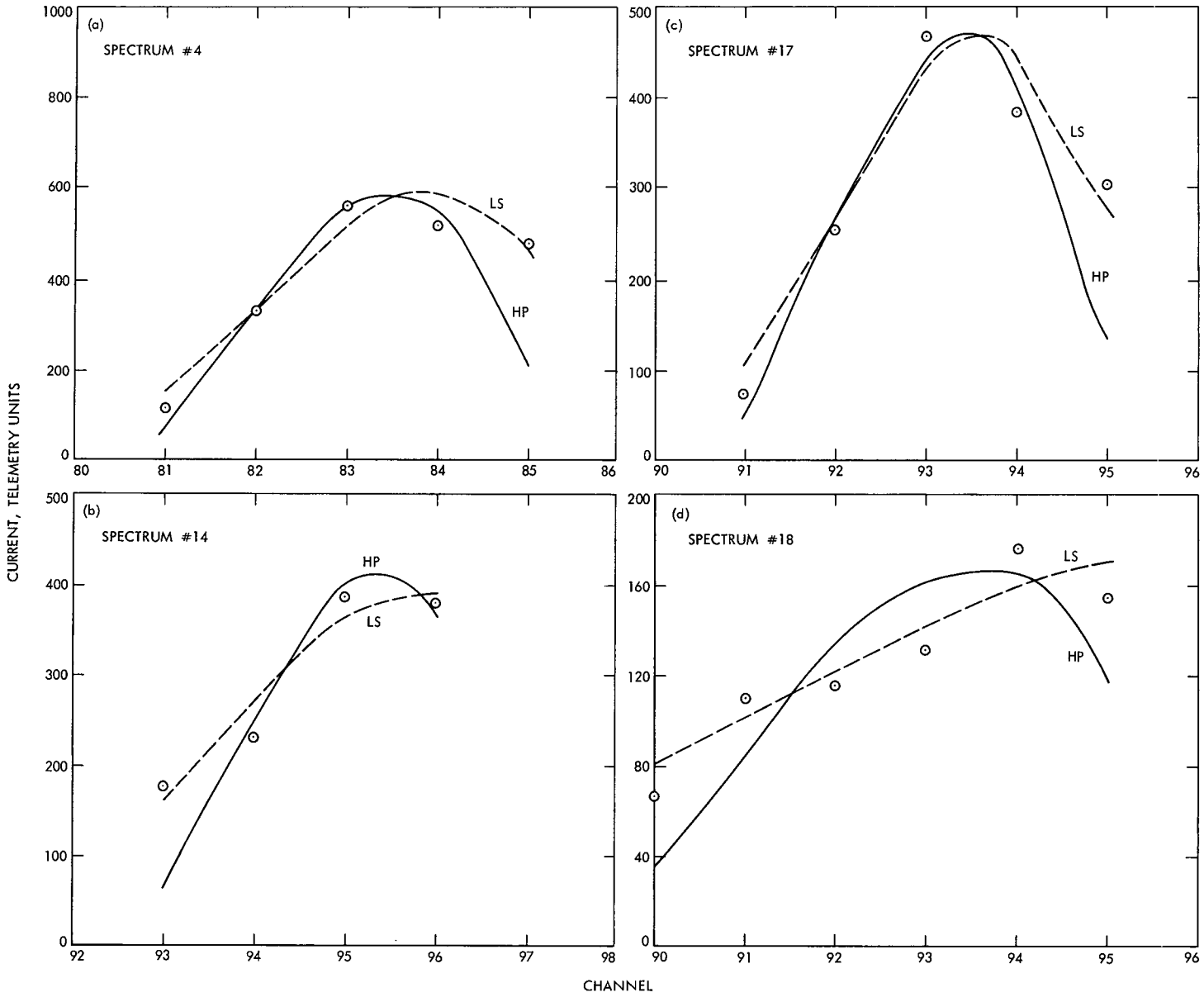

Fig. 8. Four spectra where $|\Delta T/T| > 0.20$

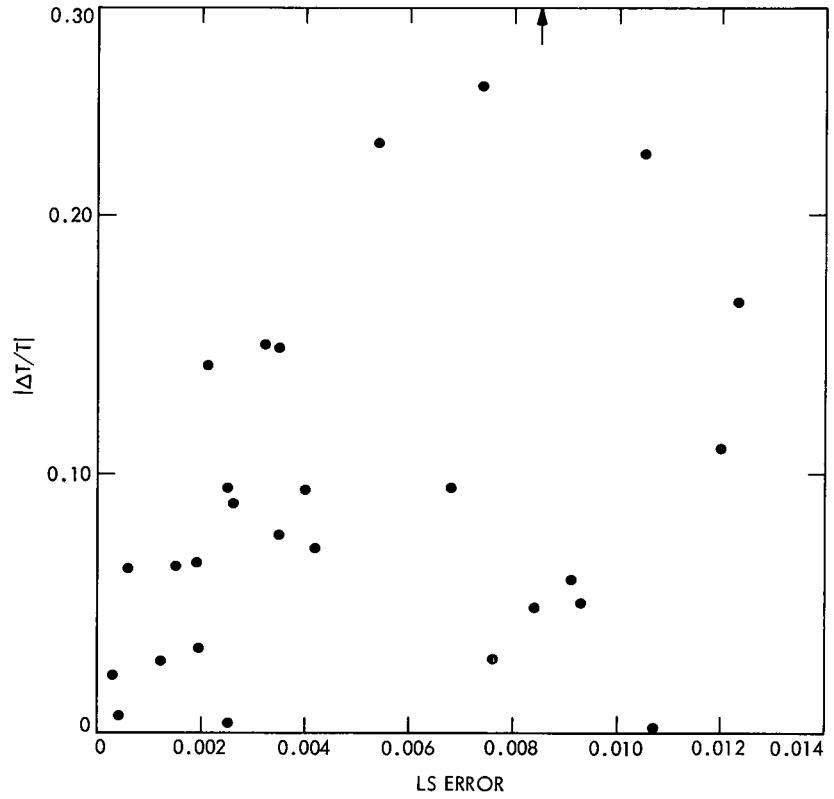

Fig. 9. $|\Delta T/T|$ vs. LS error

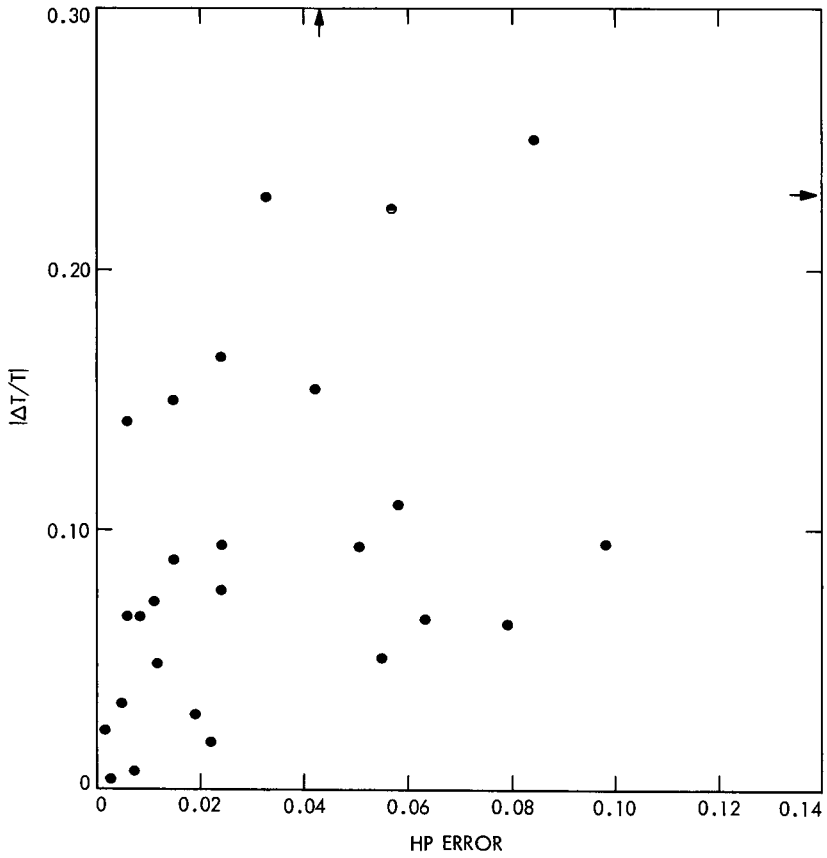

Fig. 10. $|\Delta T/T|$ vs. HP error

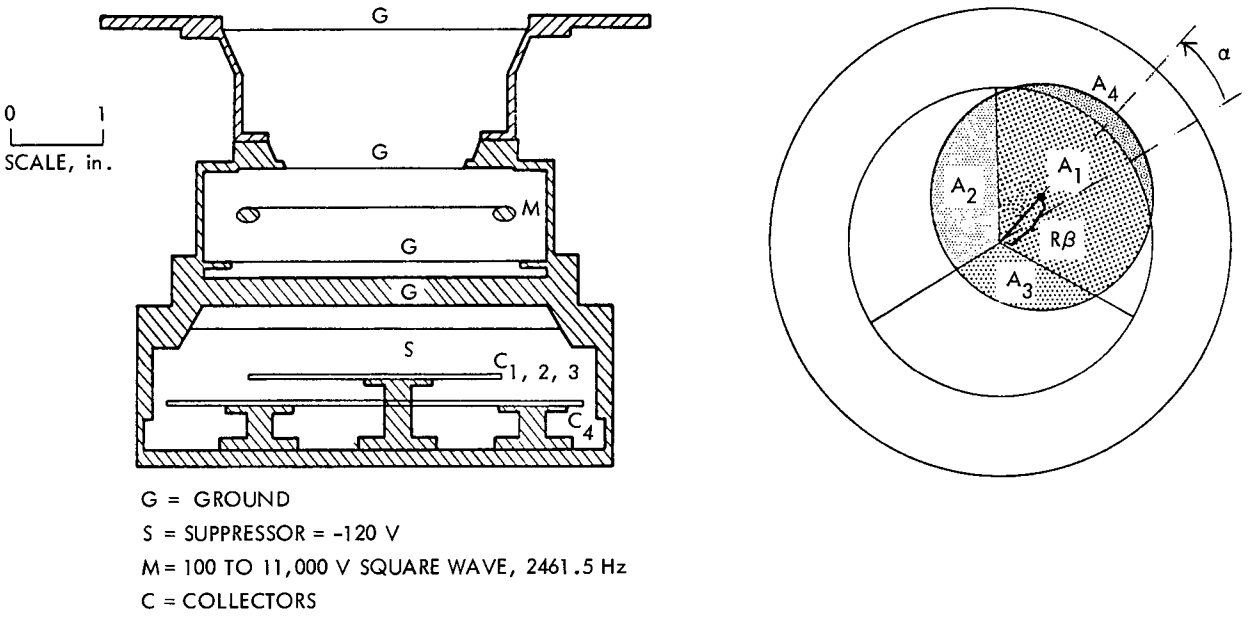

Fig. 11. OGO 5 Faraday cup detector. (Left) Scale drawing of the OGO 5 Faraday cups. (Right) Arrangement of the four current collectors in the OGO 5 Faraday cups and the impact location (shaded areas) for a beam of particles entering the instrument from a direction corresponding to the angles α and β.

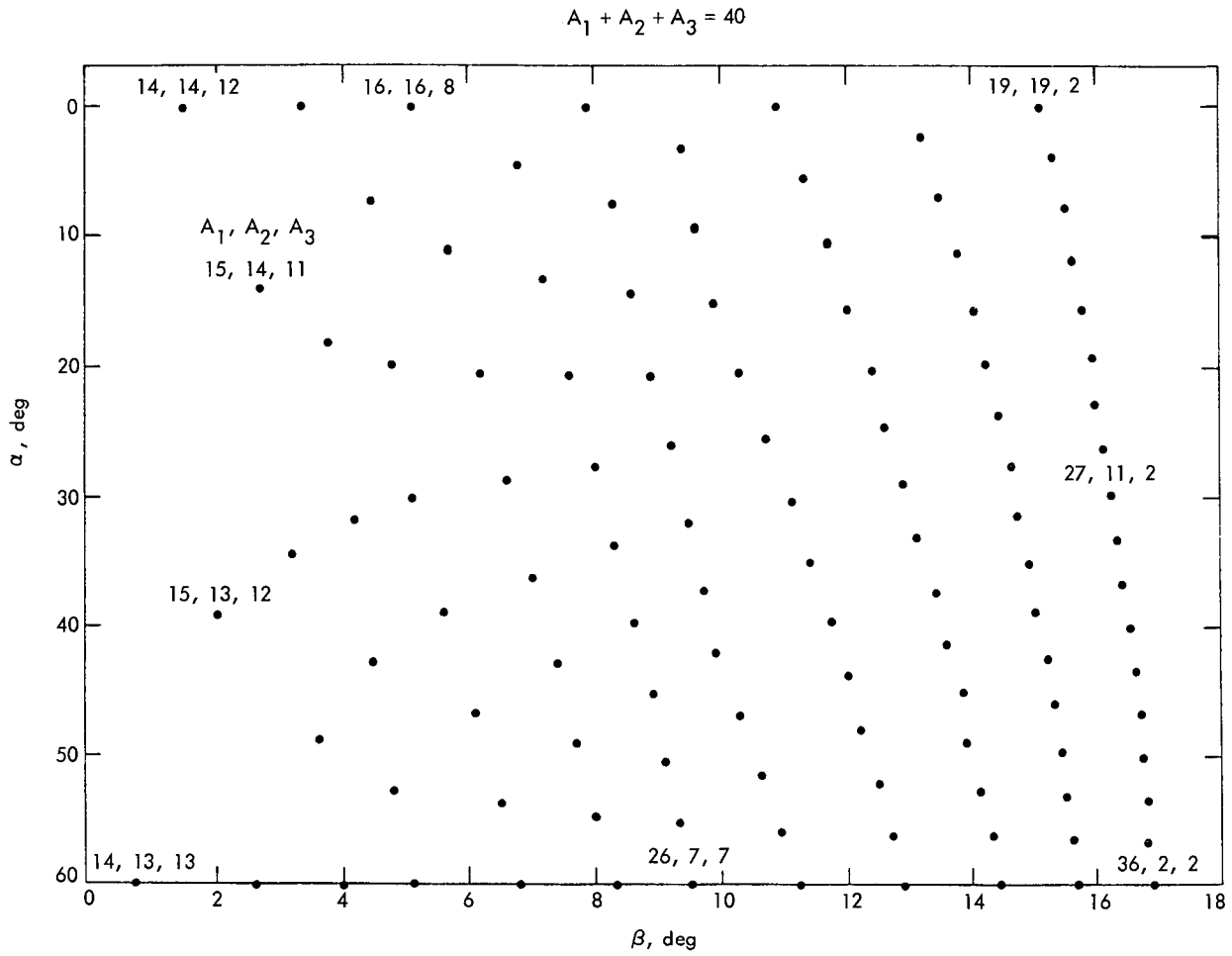

Fig. 12. Values of the angles α and β as a function of the relative currents A_1, A_2, and A_3 to collectors C_1, C_2, and C_3, respectively. The spacing of points in this figure indicate the uncertainties in α and β arising from the digitization of the current measurements for the particular case $A_1 + A_2 + A_3 = 40$ telemetry units.

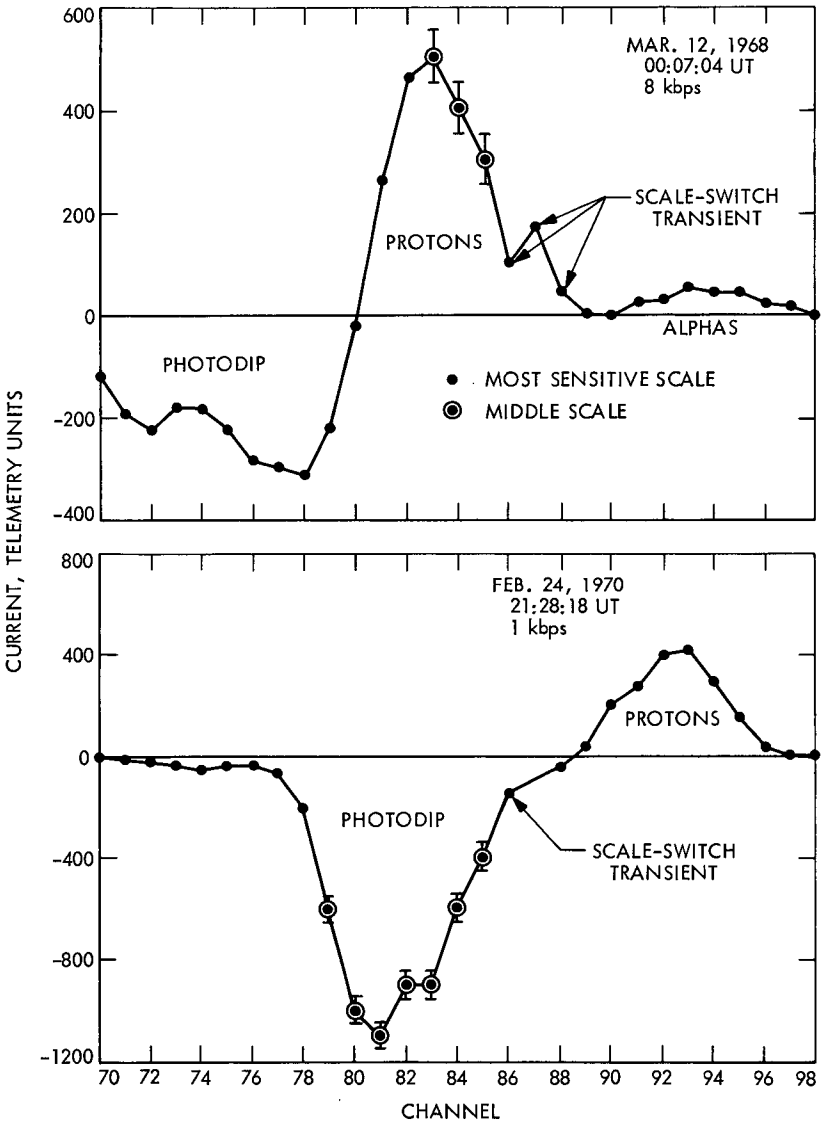

Fig. 13. Sample curved-plate analyzer spectra